The Abdus Salam
International Centre for Theoretical Physics

United Nations
Educational, Scientific and
Cultural Organization

IAEA
International Atomic Energy Agency

2328-3

Preparatory School to the Winter College on Optics and the Winter College on Optics: Advances in Nano-Optics and Plasmonics

30 January - 17 February, 2012

Nanoplasmonics: Optical Properties of Plasmonic Nanosytems I

M.I. Stockmani
Georgia State University
Atlanta
U.S.A.

Department of Physics and Astronomy
Georgia State University
Atlanta, GA 30303-3083

Support: US Israel Binational Science Foundation

Nanoplasmonics: Optical Properties of Plasmonic Nanosystems

Mark I. Stockman

Department of Physics and Astronomy, Georgia State University, Atlanta, GA 30303, USA

Lecture 1:

Introduction to Nanoplasmonics. Plasmon Polaritonics: Propagation of Surface Plasmon Polaritons in Nanostructured Systems

Meet the Author
in his natural
environment:

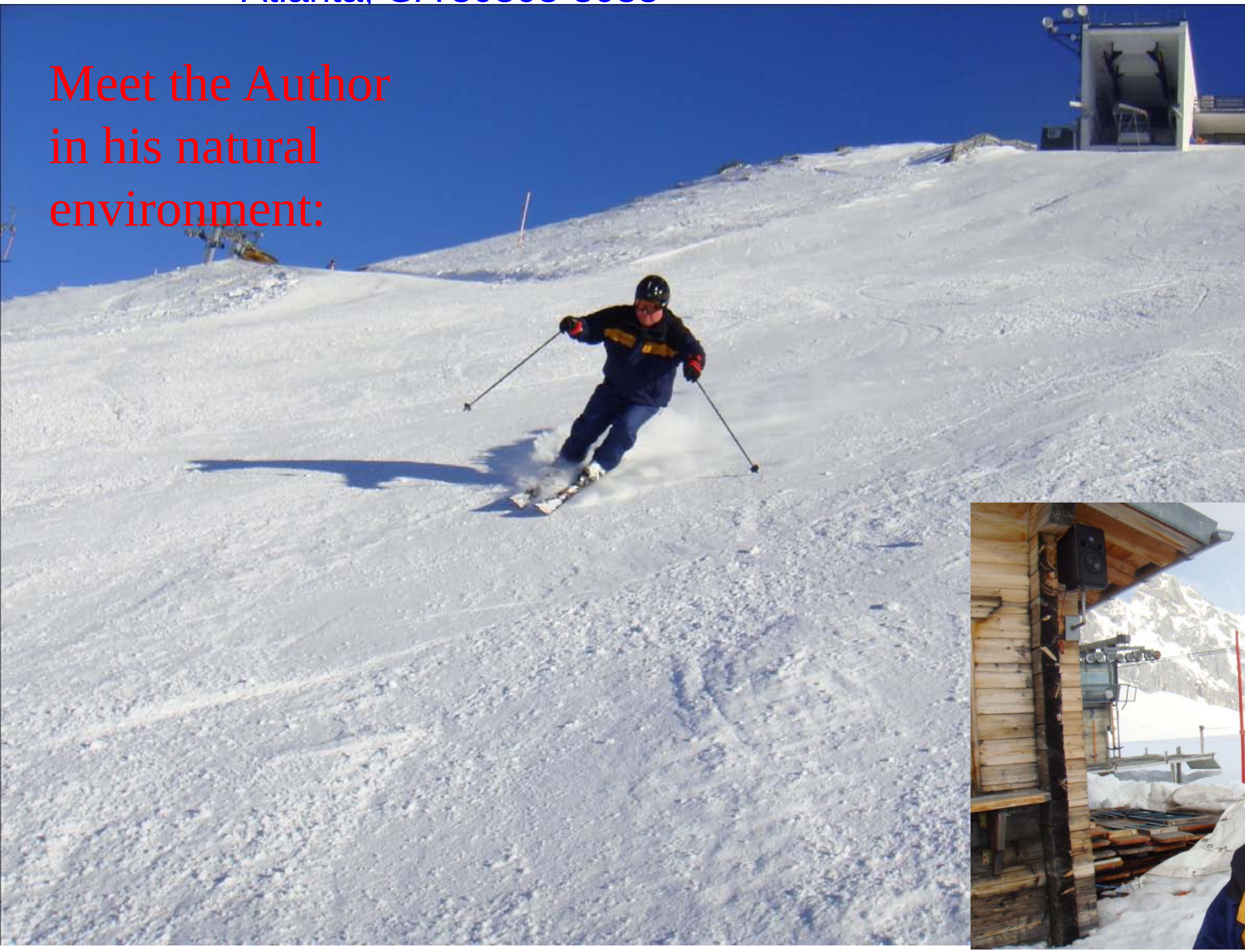

CONTENTS OF THE COURSE

• Lecture 1: **Introduction to Nanoplasmonics. Plasmon Polaritonics: Propagation of Surface Plasmon Polaritons in Nanostructured Systems**

•Lecture 2: **Nanoplasmonics of Nanosystems: Localized Surface Plasmon Resonances**

•Lecture 3: **Ultrafast, Nonlinear, and Quantum Nanoplasmonics**

Collaborators (alphabetical ordering):

1. David J. Bergman, Department of Physics, Tel Aviv University, Israel
2. Sophie Brasselet, Institut Fresnel, Marseilles, France
3. Paul Corkum, Femtosecond Science Program, National Research Council of Canada
4. Maxim Durach, Georgia State University, Atlanta, USA
5. Sergey V. Faleev, Sandia National Laboratories, Livermore, CA, USA
6. Harald Giessen, University of Stuttgart, Germany
7. Dmitry Gramotnev, Queensland University of Technology, Brisbane, Australia
8. Misha Ivanov, Femtosecond Science Program, National Research Council of Canada
9. Ulf Kleineberg, Ludwig Maximilian University, Munich, Germany
10. Victor Klimov, Los Alamos National Laboratory, Los Alamos, New Mexico, USA
11. Matthias Kling, Max Plank Institute for Quantum Optics, Garching, Germany
12. Katrin Kneipp, Danish Technical University, Copenhagen, Denmark
13. Takayoshi Kobayashi, University of Tokyo
14. Ferenc Krausz, Max Plank Institute for Quantum Optics, Garching, Germany
15. Ivan Larkin, Georgia State University, Atlanta, GA, USA
16. Kuiru Li, Georgia State University, Atlanta, USA
17. Keith Nelson, MIT, Boston, MA, USA
18. Peter Nordlander, Rice University, Houston, Texas, USA
19. Hrvoje Petek, University of Pittsburgh, USA
20. Anastasia Rusina, Georgia State University, Atlanta,, USA
21. Igor Tsukerman, University of Akron, USA
22. Nikolay Zheludev, University of Southampton, UK
23. Joseph Zyss, Ecole Normale Supérieure de Cachan, France

LECTURE 1

Introduction to Nanoplasmonics.

Plasmon Polaritonics: Propagation of Surface Plasmon Polaritons in Nanostructured Systems

1. Introduction
    - Problem of nanolocalization of energy
    - Surface plasmons and enhanced optical fields
    - Applications of surface plasmonics
2. Surface plasmon polaritons as interface electromagnetic waves
    - Maxwell equations solution for metal-dielectric interface
    - Surface plasmon polaritons in layered media
3. Adiabatic energy concentration in tapered plasmonic waveguides: theory and experiment
4. Negative refraction in nanoplasmonic waveguides (optional)

Department of Physics and Astronomy
Georgia State University
Atlanta, GA 30303-3083

PROBLEMS IN NANOOPTICS

Microscale

Delivery of energy to nanoscale: Conversion of propagating EM wave to local fields

Enhancement and control of local nanoscale fields. Enhanced near-field responses

Ultrafast, nonlinear, and quantum nanoplasmonics (SPASER)

Department of Physics and Astronomy
Georgia State University
Atlanta, GA 30303-3083

Concentration of optical **(electromagnetic wave)** energy: Minimum size of electromagnetic wave in uniform space

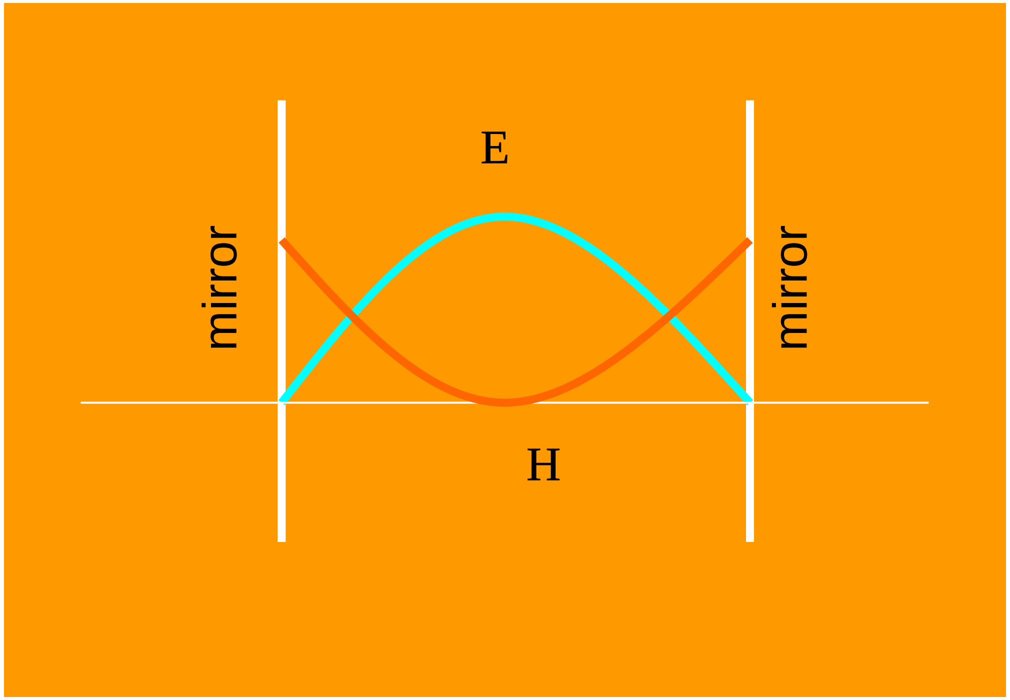

Departn
Georgia
Atlanta,

Nanoplasmonics in a nano-nutshell

Reduced wavelength, ~100 nm

Enhanced Local Fields in Proximity of Metal Nanoparticle are Nanoscale-Localized

Mean free path, ~40 nm

Skin depth, ~25 nm

Nanoplasmonics: ~10 nm

v_F/ω Spatial dispersion/Nonlocality radius, ~1 nm

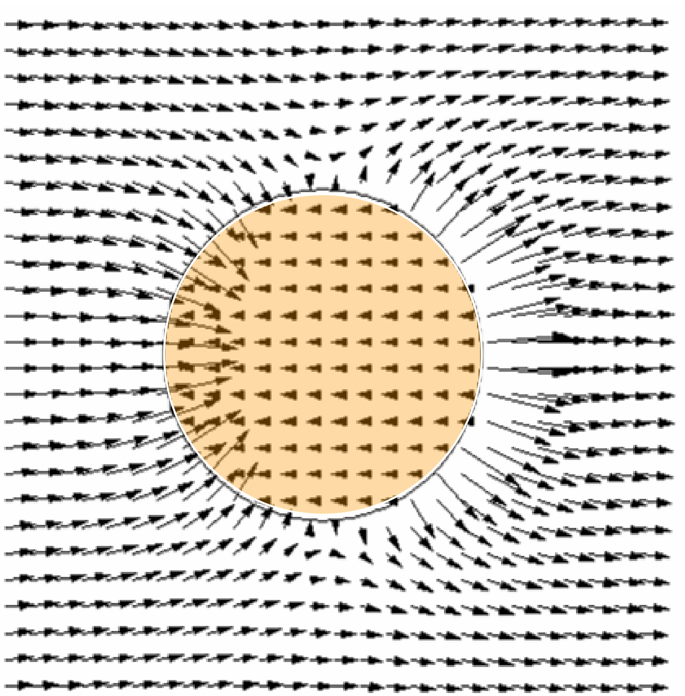

Polarizability:

$$\alpha = R^3 \frac{\varepsilon_m - \varepsilon_d}{\varepsilon_m + 2\varepsilon_d}$$

Field enhancement or Quality factor:

$$Q = \frac{-\operatorname{Re}\varepsilon_m}{\operatorname{Im}\varepsilon_m} \sim 10-100$$

Localized Surface Plasmon:

Lattice

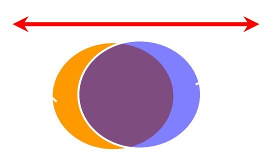

Electrons

Department of Physics and Astronomy
Georgia State University
Atlanta, GA 30303-3083

Lycurgus Cup (4th Century AD): Roman Nanotechnology

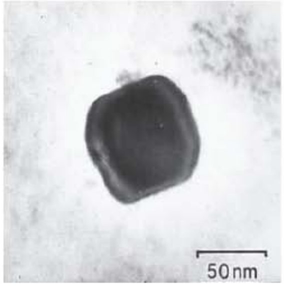

I. Freestone, N. Meeks, M. Sax, and C. Higgitt, *The Lycurgus Cup - a Roman Nanotechnology*, Gold Bull. **40**, 270-277 (2007)

Nanoplasmonic colors are very bright. Scattering and absorption of light by them are very strong. This is due to the fact that all of the millions of electrons move in unison in plasmonic oscillations

Nanoplasmonic colors are also eternal: metal nanoparticles are stable in glass: they do not bleach and do not blink. Gold is stable under biological conditions and is not toxic *in vivo*

Colors of Silver Nanocrystals and Gold Nanoshapes

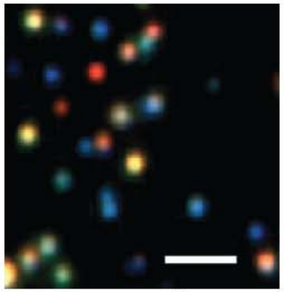

2 µm

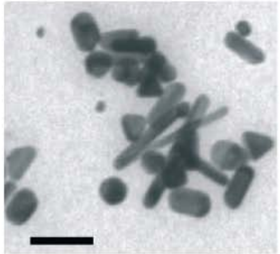

100 nm

C. Orendorff, T. Sau, and C. Murphy, *Shape-Dependent* …, Small **2**, 636-639 (2006)

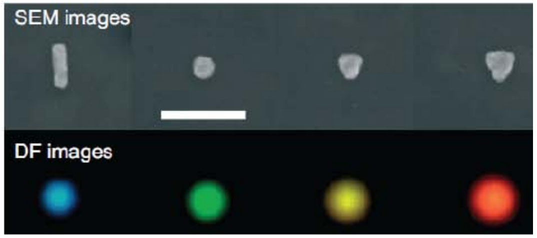

Scanning electron microscopy

Dark field optical microscopy

W. A. Murray and W. L. Barnes, *Plasmonic Materials*, Adv. Mater. **19**, 3771-3782 (2007) [Scale bar: 300 nm]

Eternal nanoplasmonic colors (Notre Dame de Paris)


The most beautiful polychroic nanoplasmonic colors of the world: La Sainte Chapelle, Paris

Department of Physics and Astronomy
Georgia State University
Atlanta, GA 30303-3083

Department of Physics and Astronomy
Georgia State University
Atlanta, GA 30303-3083

Plasmonic Hot Spots

Happy17th Anniversary!

- D. P. Tsai *et al.*, *Phys. Rev. Lett.* **72**, 4149 (1994)
- M. I. Stockman et al., *Phys. Rev. Lett.* **75**, 2450 (1995)
- M. I. Stockman, L. N. Pandey, and T. F. George, Phys. Rev. B **53**, 2183-2186 (1996)

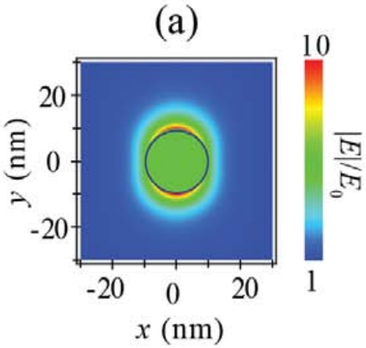

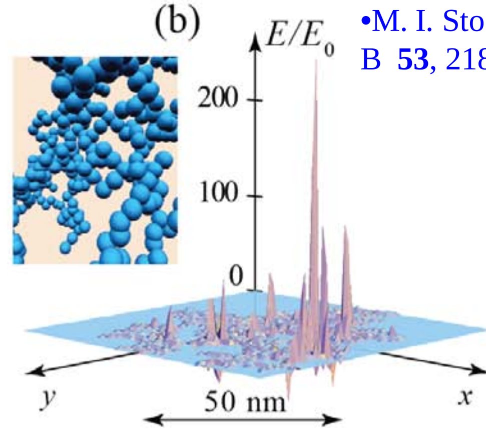

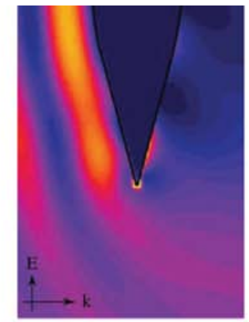

L. Novotny and S. J. Stranick, Annual Rev. Phys. Chem. **57**, 303-331 (2006)

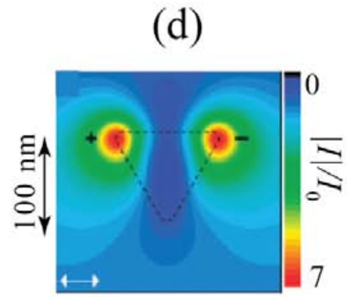

M. Rang et al., Nano Lett. **8**, 3357 (2008)

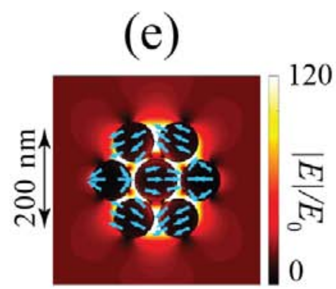

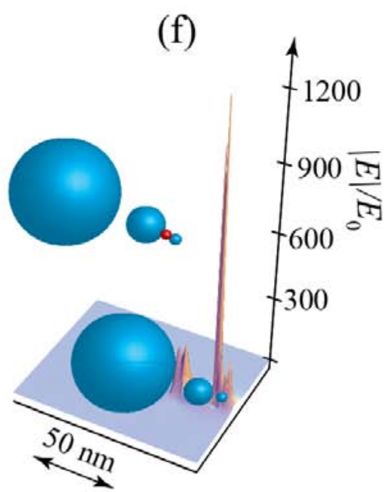

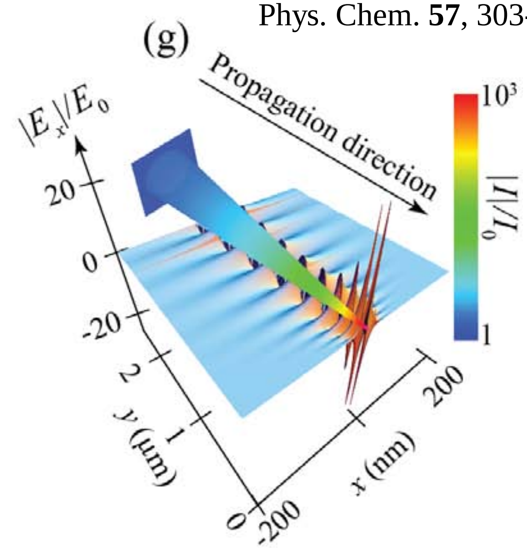

- J. A. Fan et al., Science **328**, 1135 (2010)
- M. Hentschel et al., Nano Lett. **10**, 2721 (2010)

K. Li, M. I. Stockman, and D. J. Bergman, Phys. Rev. Lett. **91**, 227402 (2003)

M. I. Stockman, Phys. Rev. Lett. **93**, 137404 (2004)

Department of Physics and Astronomy
Georgia State University
Atlanta, GA 30303-3083

A. Kubo, K. Onda, H. Petek, Z. Sun, Y. S. Jung, and H. K. Kim, *Femtosecond Imaging of Surface Plasmon Dynamics in a Nanostructured Silver Film*, Nano Lett. 5, 1123 (2005).

200 nm

30 femtoseconds from life of a nanoplasmonic systems

Localized SP hot spots are deeply subwavelength as seen in PEEM (photoemission electron microscope)

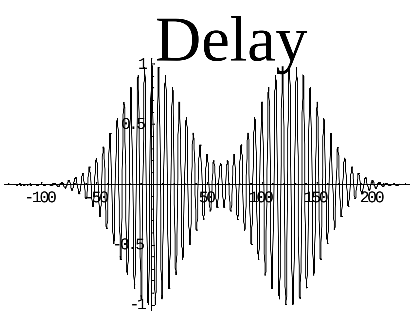

PEEM Image as a Function of Delay (250 as per frame)

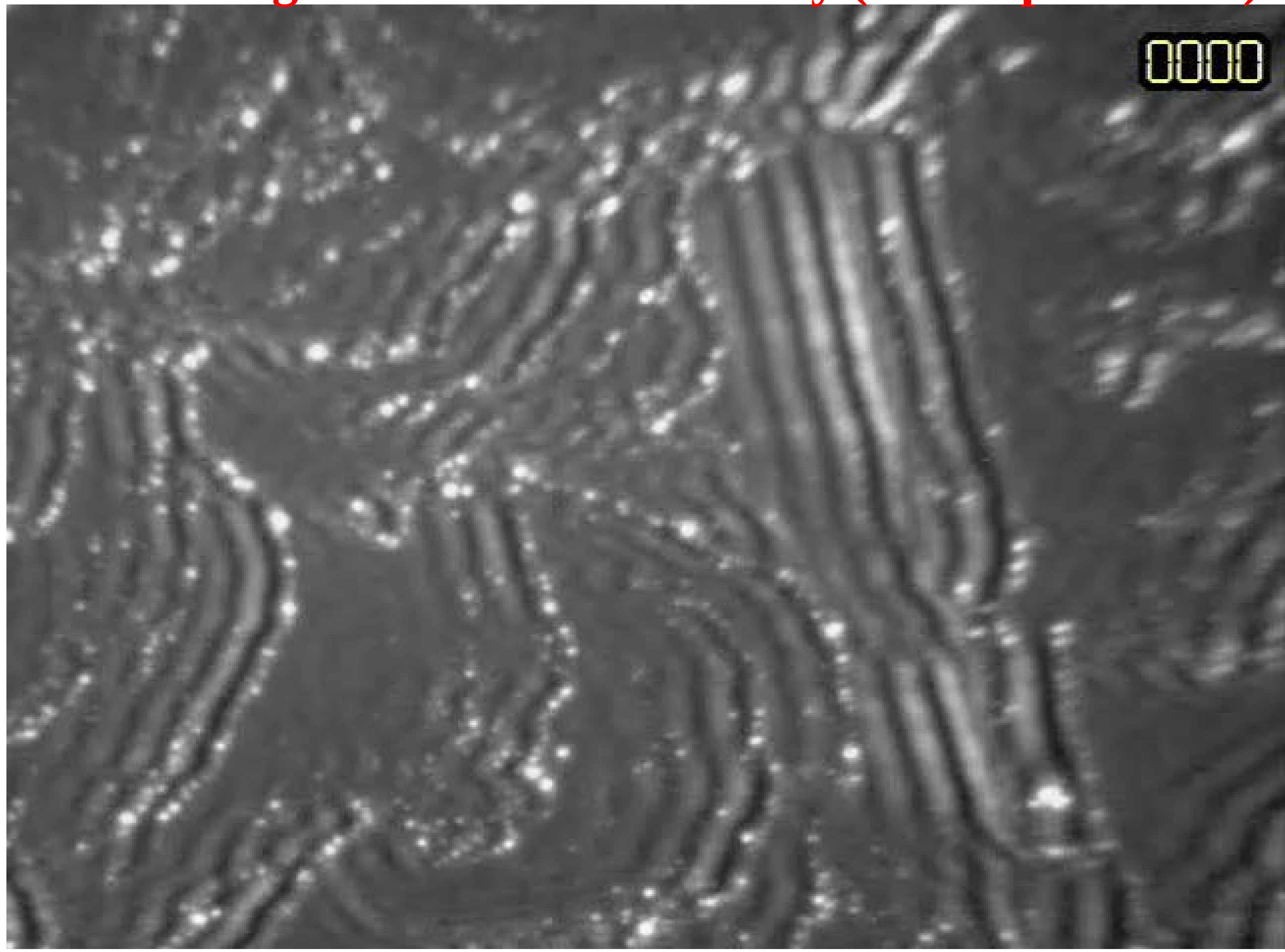

Applications of Nanoplasmonics:

1. Ultrasensitive and express sensing and detection using both SPPs and SPs (LSPRs): see,e.g., J. N. Anker, W. P. Hall, O. Lyandres, N. C. Shah, J. Zhao, and R. P. Van Duyne, *Biosensing with Plasmonic Nanosensors*, Nature Materials 7, 442-453 (2008);
2. NSOM (SNOM)
3. Nanoantennas: Coupling of light to nanosystems. Extraction of light from LEDs and lasers [N. F. Yu, J. Fan, Q. J. Wang, C. Pflugl, L. Diehl, T. Edamura, M. Yamanishi, H. Kan, and F. Capasso, *Small-Divergence Semiconductor Lasers by Plasmonic Collimation*, Nat. Phot. 2, 564-570 (2008)]; nanostructured antennas for photodetectors and solar cells; heat-assisted magnetic memory [W. A. Challener *et al.*, Nat. Photon. 3, 220 (2009)]
4. Photo- and chemically stable labels and probes for biomedical research and medicine
5. Nanoplasmonic-based immunoassays and tests. Home pregnancy test (dominating the market), PSA test (clinic), troponin heart-attack test, and HIV tests (in trials)
6. Near perspective: Generation of EUV and XUV pulses
7. Thermal cancer therapy: L. R. Hirsch, R. J. Stafford, J. A. Bankson, S. R. Sershen, B. Rivera, R. E. Price, J. D. Hazle, N. J. Halas, and J. L. West, *Nanoshell-Mediated Near-Infrared Thermal Therapy of Tumors under Magnetic Resonance Guidance*, Proc. Natl. Acad. Sci. USA 100, 13549-13554 (2003). C. Loo, A. Lowery, N. Halas, J. West, and R. Drezek, *Immunotargeted Nanoshells for Integrated Cancer Imaging and Therapy*, Nano Lett. 5, 709-711 (2005)

Department of Physics and Astronomy
Georgia State University
Atlanta, GA 30303-3083

Nanosensors based on enhanced local fields

Surface plasmon frequency shifts to red upon molecules adhesion

$$\omega_p = \frac{\omega_{0p}}{\sqrt{\varepsilon_h}}$$

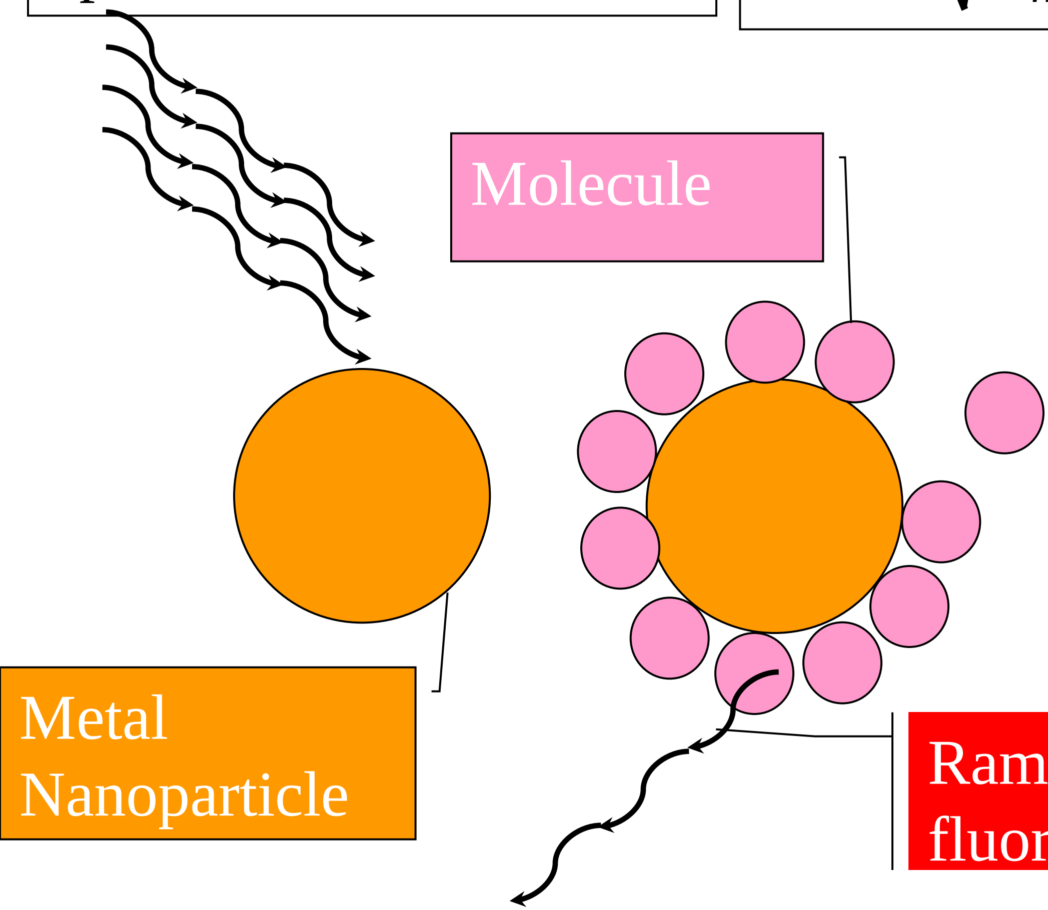

- X. Zhang, M. A. Young, O. Lyandres, and R. P. Van Duyne, *Rapid Detection of an Anthrax Biomarker by Surface-Enhanced Raman Spectroscopy*, Journal of American Chemical Society **127**, 4484 (2005).
- C. R. Yonzon, C. L. Haynes, X. Y. Zhang, J. T. Walsh, and R. P. Van Duyne, *A Glucose Biosensor Based on Surface-Enhanced Raman Scattering*, Anal. Chem. **76**, 78-85 (2004).

Use of Enhanced Local Fields for Nano-Microscopy

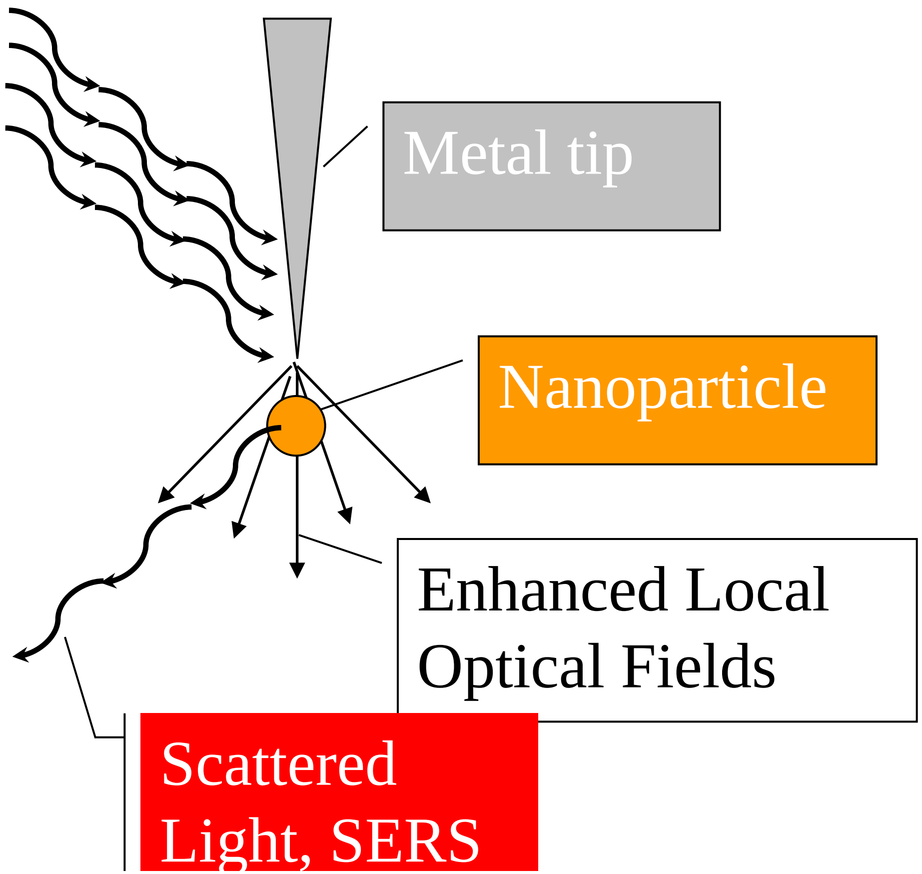

- L. Novotny and S. J. Stranick, *Near-Field Optical Microscopy and Spectroscopy with Pointed Probes*, Annual Rev. Phys. Chem. **57**, 303-331 (2006).
- A. Hartschuh, E. J. Sanchez, X. S. Xie, and L. Novotny, *High-Resolution Near-Field Raman Microscopy of Single-Walled Carbon Nanotubes*, Phys. Rev. Lett. **90**, 095503 -1-4 (2003).

NANONICS IMAGING Ltd.

NSOM images of healthy human dermal fibroblasts in liquid obtained in transmission mode with a Nanonics cantilevered tip with a gold nanosphere

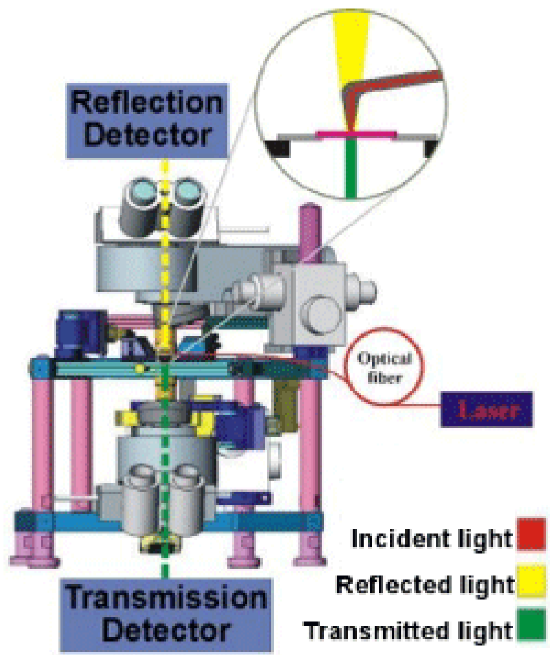

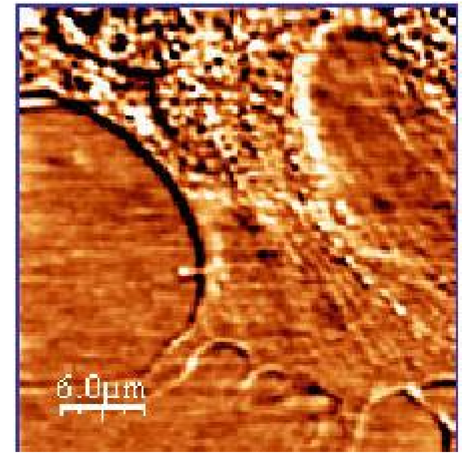

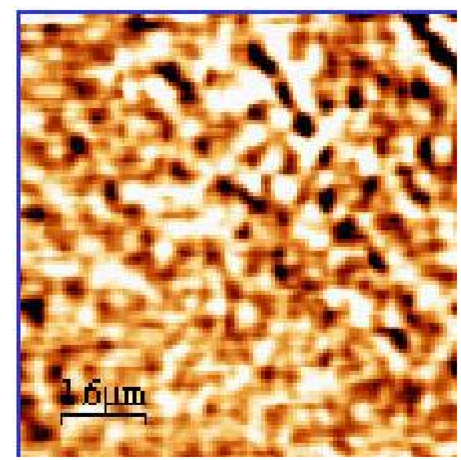

Department of Physics and Astronomy
Georgia State University
Atlanta, GA 30303-3083

NeuroImage 49 (2010) 517–524

Contents lists available at ScienceDirect

NeuroImage

journal homepage: www.elsevier.com/locate/ynimg

Novel approaches for scanning near-field optical microscopy imaging of oligodendrocytes in culture

E. Trevisan [a], E. Fabbretti [b,c], N. Medic [d], B. Troian [e], S. Prato [e], F. Vita [f], G. Zabucchi [d], M. Zweyer [a,*]

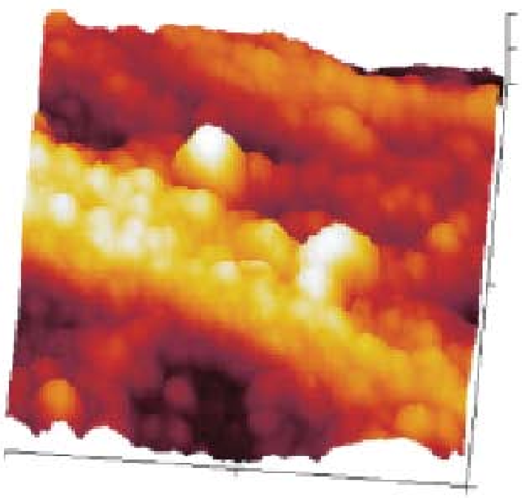

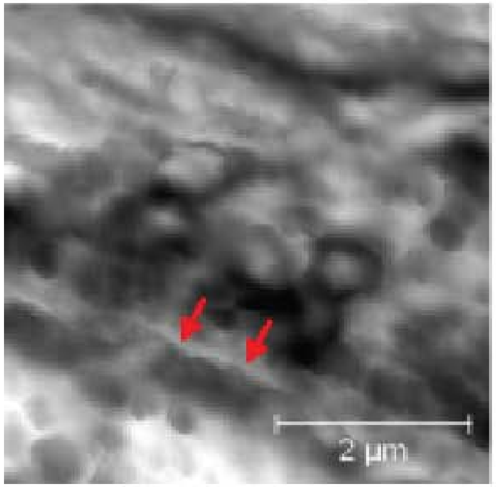

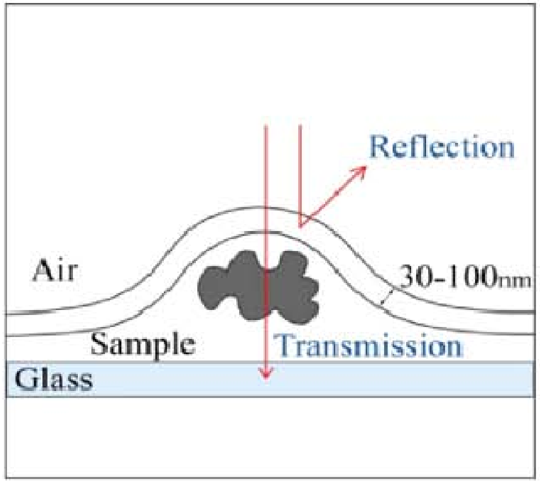

Department of Physics and Astronomy
Georgia State University
Atlanta, GA 30303-3083

Chirality Changes in Carbon Nanotubes Studied with Near-Field Raman Spectroscopy

Neil Anderson, Achim Hartschuh, and Lukas Novotny

Nano Lett. 577 – 582 (2007); DOI: 10.1021/nl0622496

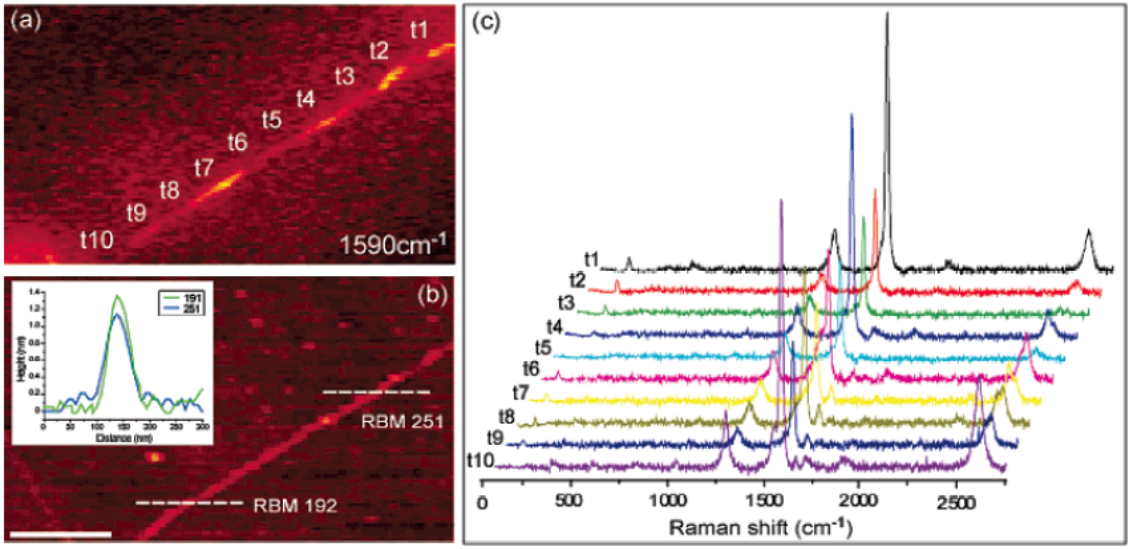

Figure 1. Near-field Raman imaging and spectroscopy: near-field Raman image (a) and corresponding topography image (b) of an isolated SWNT, where the optical resolution was determined to be 40 nm (fwhm). Also shown are a series of tip-enhanced Raman spectra (c) acquired along the length of the SWNT. From the recorded spectra, two resonant RBM phonons are detected. One RBM phonon frequency is detected at 251 cm^{-1}, from which we assign a semiconducting chirality. The second RBM phonon frequency recorded from the lower section of the SWNT is centered at 192 cm^{-1}, from which we assign a metallic chirality. See main text for details. The inset of (b) displays two cross-sectional profiles acquired from both the upper and lower sections, respectively, revealing that the expected diameter change occurs as the SWNT undergoes the transition from a semiconducting to metallic chirality. Scale bar denotes 200 nm and is valid for both (a) and (b).

Department of Physics and Astronomy
Georgia State University
Atlanta, GA 30303-3083

Next generation of scanning near-field optical microscopy (SNOM) with chemical mapping:

Adiabatic concentration of optical energy and giant surface-enhanced Raman scattering (SERS); resolution 7 nm.s

(to be discussed in the course)

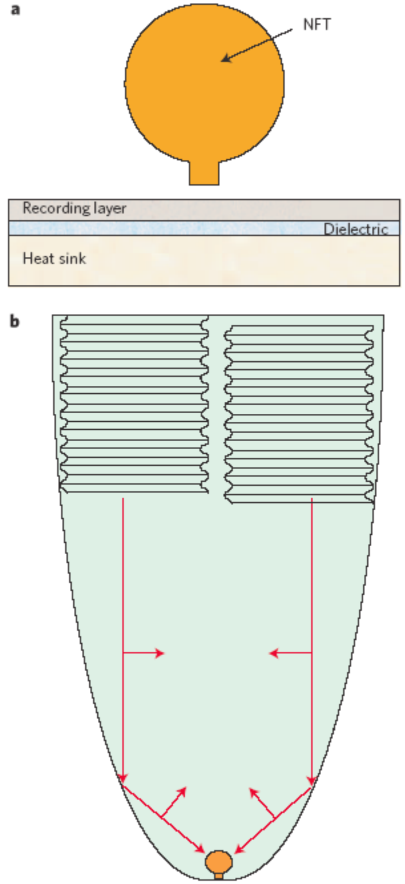

nature photonics ARTICLES
PUBLISHED ONLINE: 22 MARCH 2009 | DOI: 10.1038/NPHOTON.2009.26

Heat-assisted magnetic recording by a near-field transducer with efficient optical energy transfer

W. A. Challener*, Chubing Peng, A. V. Itagi, D. Karns, Wei Peng, Yingguo Peng, XiaoMin Yang, Xiaobin Zhu, N. J. Gokemeijer, Y.-T. Hsia, G. Ju, Robert E. Rottmayer, Michael A. Seigler and E. C. Gage

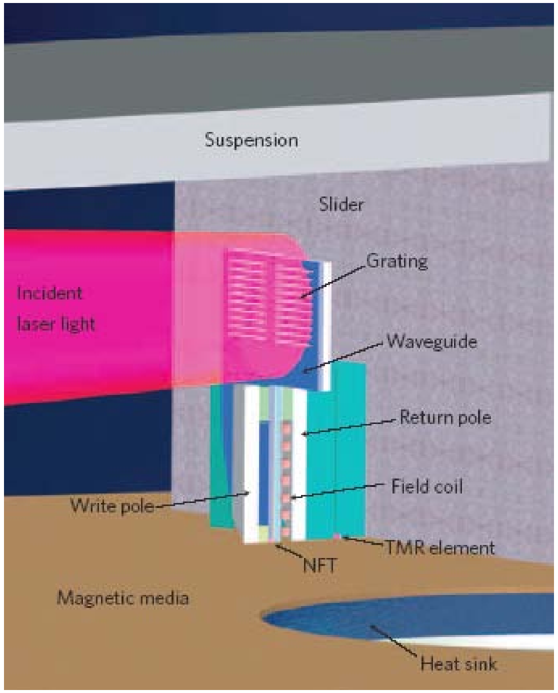

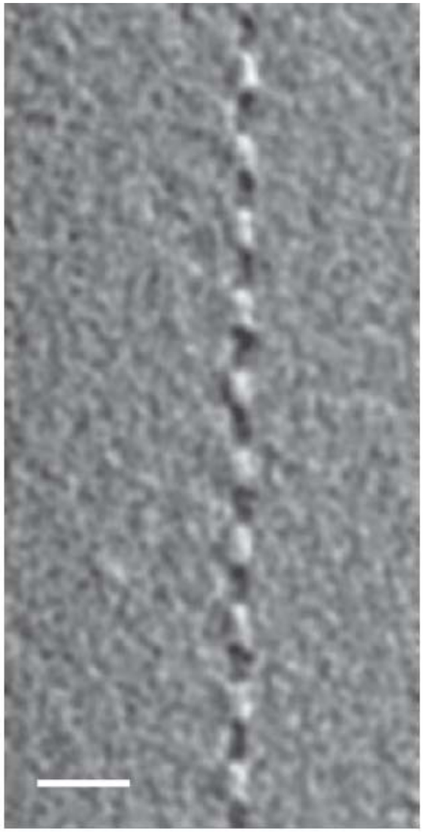

MFM image of a recorded track. The track width is ~70 300 nm.

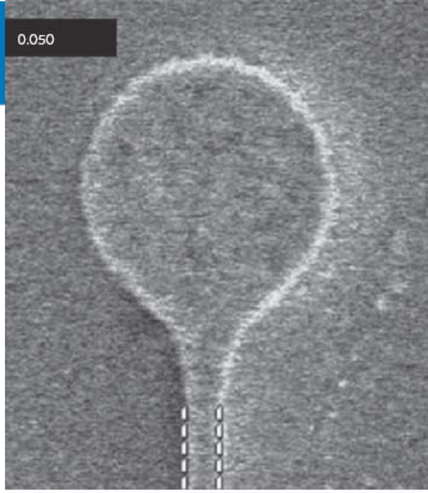

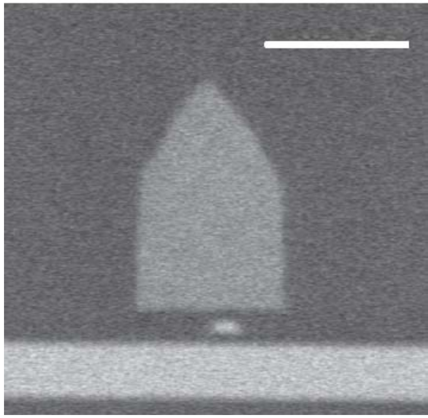

Nanometre-scale germanium photodetector enhanced by a near-infrared dipole antenna

nature photonics | VOL 2 | APRIL 2008 | www.nature.com/naturephotonics

LIANG TANG[1]*, SUKRU EKIN KOCABAS[1], SALMAN LATIF[1], ALI K. OKYAY[2], DANY-SEBASTIEN LY-GAGNON[1], KRISHNA C. SARASWAT[2] AND DAVID A. B. MILLER[1]

[1]Ginzton Laboratory, Stanford University, Stanford, California 94305, USA

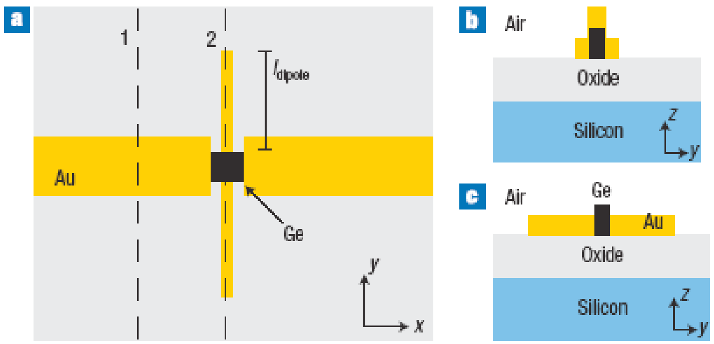

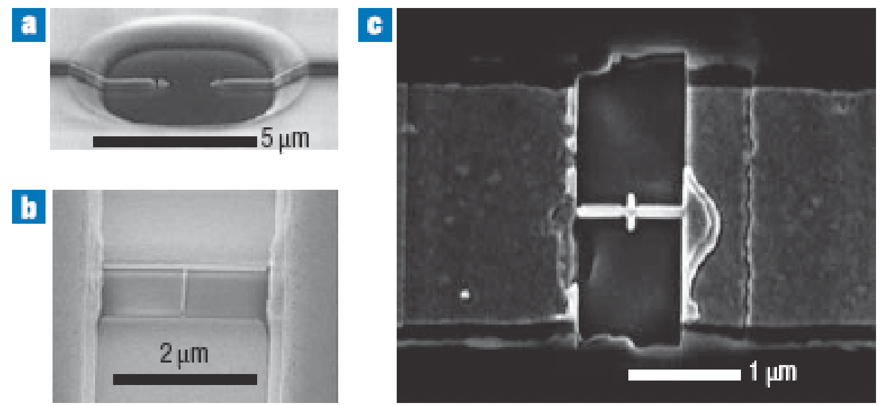

Figure 3 Scanning electron microscopy (SEM) images of the fabricated devices. a, Silicon seeding window with 2-μm-wide germanium crystalline lines. b, 60-nm-wide and 2-μm-long germanium nanowire fabricated by the first FIB step. c, An open-sleeve dipole antenna detector with $l_{dipole} = 155$ nm (this image is rotated by 90° in relation to that in b). (Charging due to a thick oxide layer limits the resolution in this SEM image.)

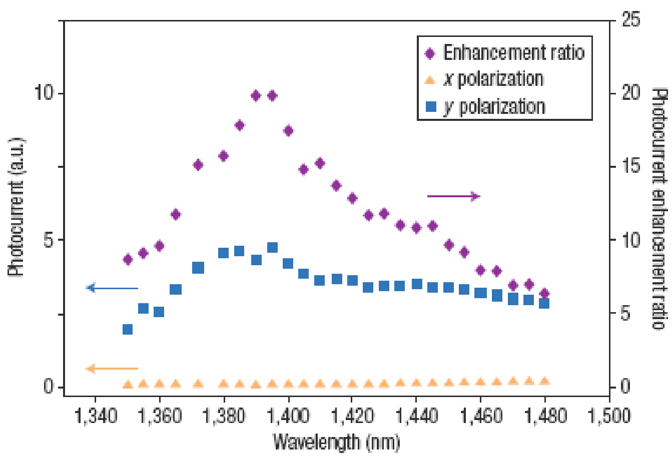

Figure 5 Measured photocurrent responses for light polarization in the y and x directions. The wavelengths were 1,350–1,480 nm for the detector with $l_{dipole} = 160$ nm.

Department of Physics and Astronomy
Georgia State University
Atlanta, GA 30303-3083

SP Sensing

1 – Antigen (hCG)
2 – Primary antibody
3 – Gold nanosphere functionalized with secondary antibody

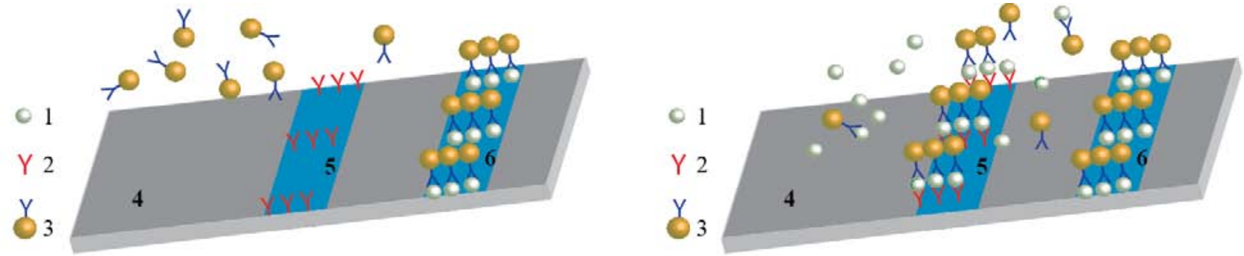

1 – Substrate
2 – Gold nanofilm
3 – Latex nanospheres
4 – Gold nanolayer
5 – Antibodies
6 - Analyte molecules

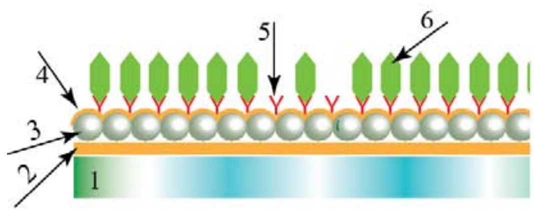

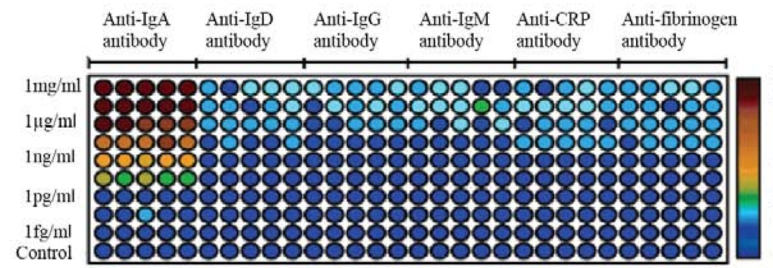

Adapted from:
T. Endo et al., Anal. Chem. **78**, 6465 (2006).

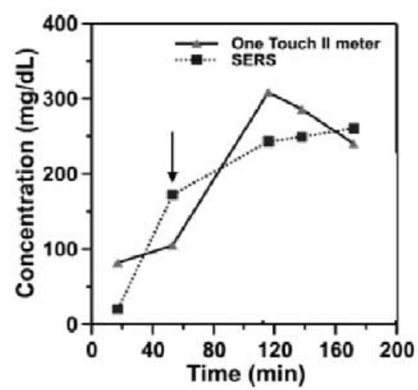

J.N. Anker et al. , Nature Materials **7**, 442 (2008)

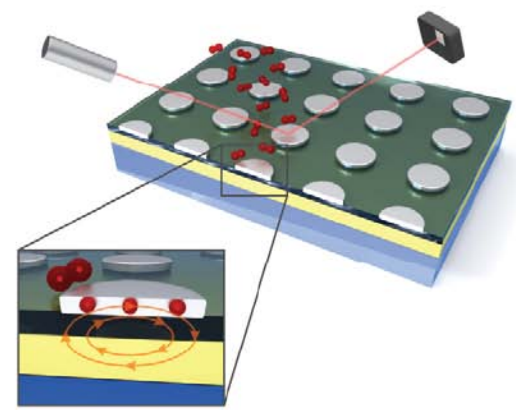

N. Liu et al., Nat. Mater. **advance online publication DOI: 10.1038/nmat3029 (2011)**

Department of Physics
Georgia State Universit
Atlanta, GA 30303-308

Vol 453|5 June 2008|doi:10.1038/nature07012 nature

LETTERS

High-harmonic generation by resonant plasmon field enhancement

Seungchul Kim[1]*, Jonghan Jin[1]*, Young-Jin Kim[1], In-Yong Park[1], Yunseok Kim[1] & Seung-Woo Kim[1]

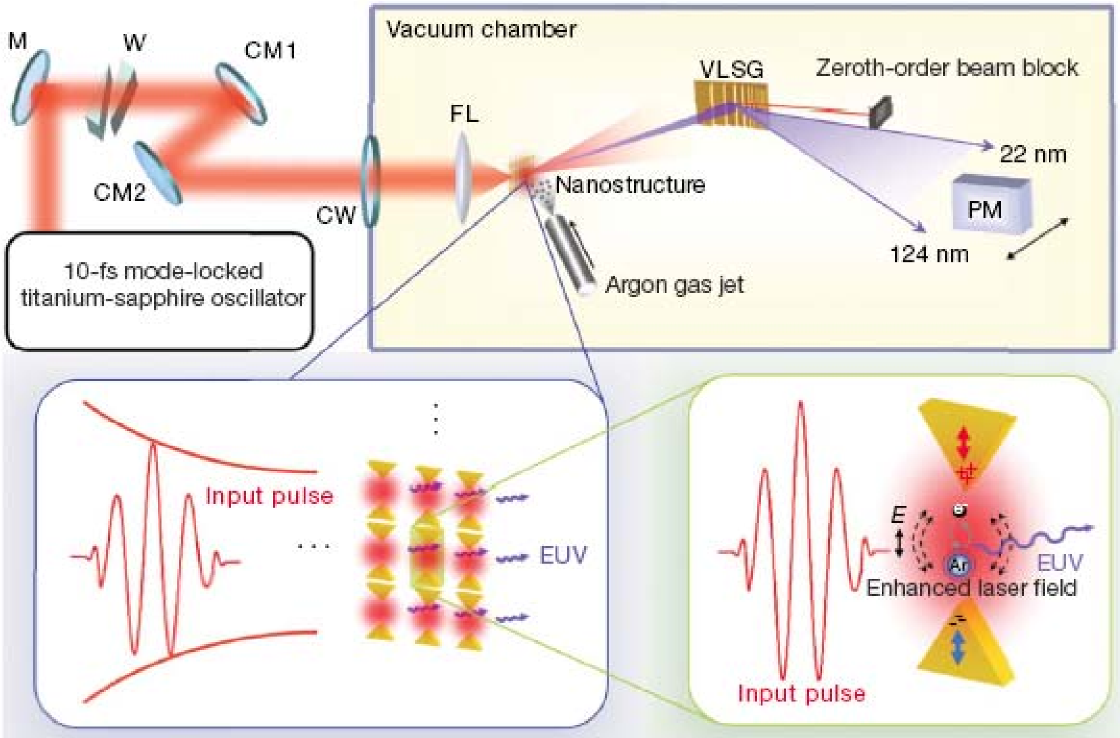

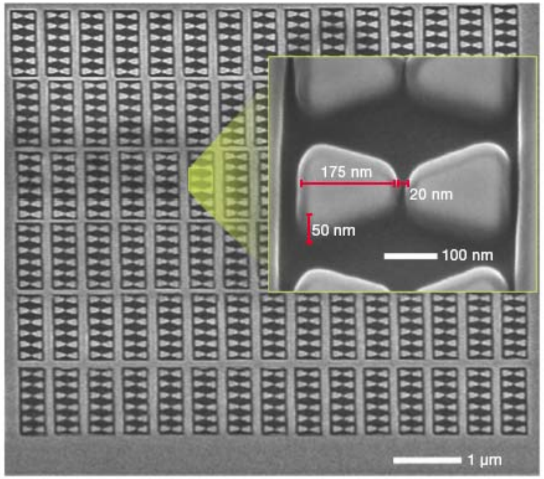

Figure 3 | Scanning electron microscope image of the nanostructure used for high-harmonic generation. Bow-tie elements were arranged in a two-

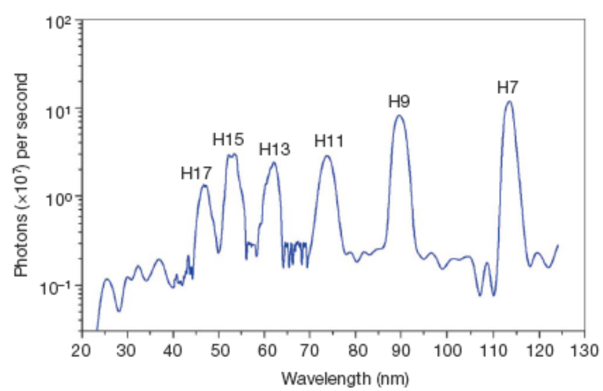

Figure 4 | Measured spectrum of generated high harmonics. A varied-line-

Georgia State University

nature photonics

LETTERS

PUBLISHED ONLINE: 16 OCTOBER 2011 | DOI: 10.1038/NPHOTON.2011.258

Plasmonic generation of ultrashort extreme-ultraviolet light pulses

In-Yong Park[1†], Seungchul Kim[1†], Joonhee Choi[1†], Dong-Hyub Lee[1], Young-Jin Kim[1], Matthias F. Kling[2], Mark I. Stockman[3] and Seung-Woo Kim[1*]

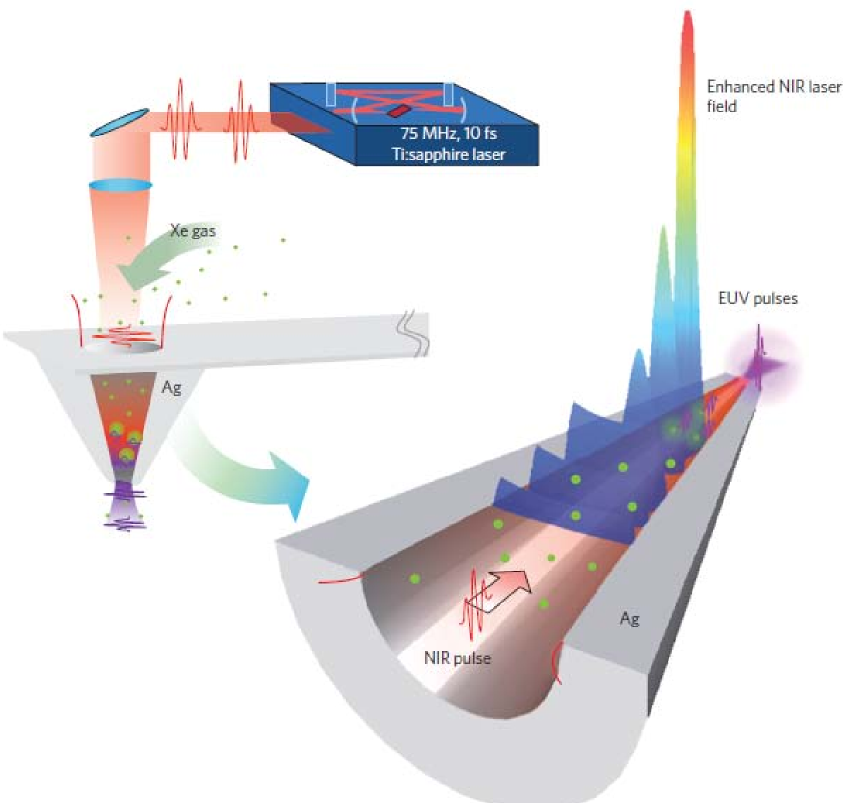

a

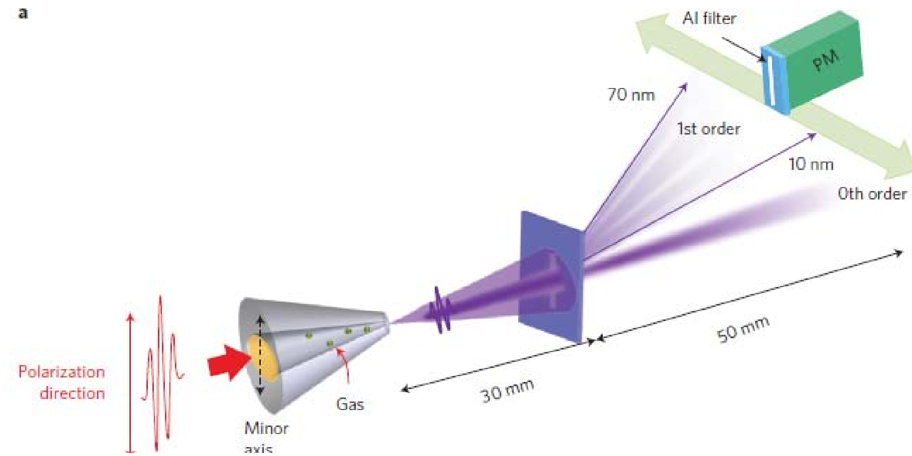

c

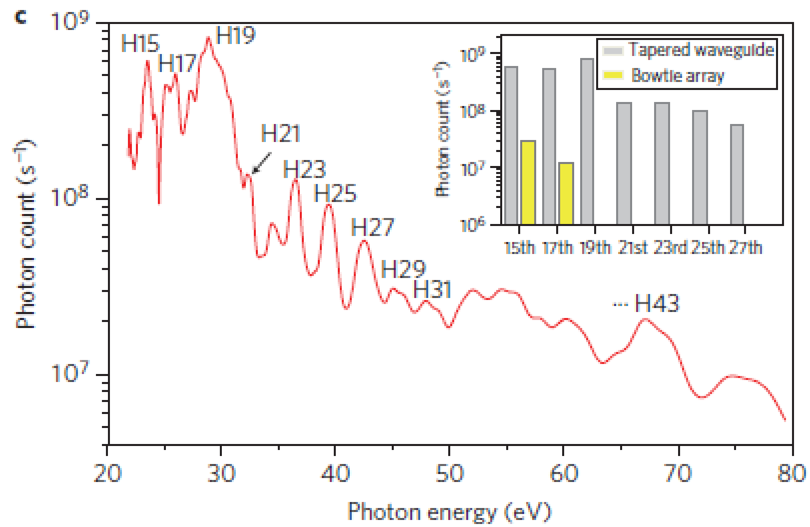

Department of Physics and Astronomy
Georgia State University
Atlanta, GA 30303-3083

insight review articles

William L. Barnes, Alain Dereux & Thomas W. Ebbesen, Nature **424**, 824 (2003)

Box 1
Surface plasmon basics

SPs at the interface between a metal and a dielectric material have a combined electromagnetic wave and surface charge character as shown in **a**. They are transverse magnetic in character (**H** is in the y direction), and the generation of surface charge requires an electric

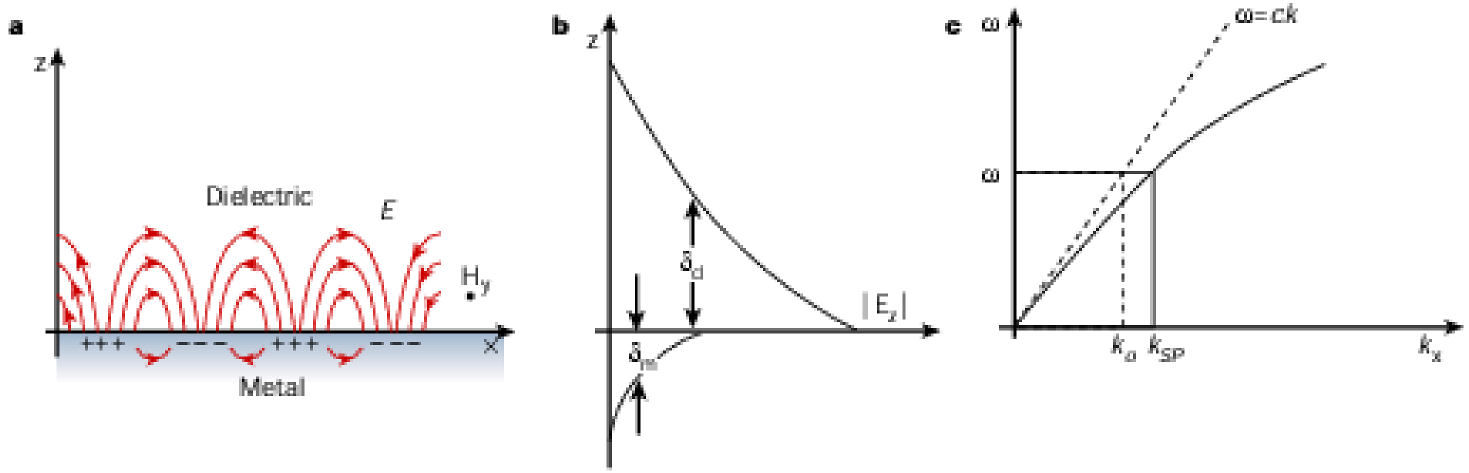

field normal to the surface. This combined character also leads to the field component perpendicular to the surface being enhanced near the surface and decaying exponentially with distance away from it (**b**). The field in this perpendicular direction is said to be evanescent, reflecting the bound, non-radiative nature of SPs, and prevents power from propagating away from the surface. In the dielectric medium above the metal, typically air or glass, the decay length of the field, δ_d, is of the order of half the wavelength of light involved, whereas the decay length into the metal, δ_m, is determined by the skin depth. **c**, The dispersion curve for a SP mode shows the momentum mismatch problem that must be overcome in order to couple light and SP modes together, with the SP mode always lying beyond the light line, that is, it has greater momentum ($\hbar k_{SP}$) than a free space photon ($\hbar k_0$) of the same frequency ω.

SURFACE PLASMON POLARITONS

Assume that we have a plane interface and consider propagation in the *xy* plane.

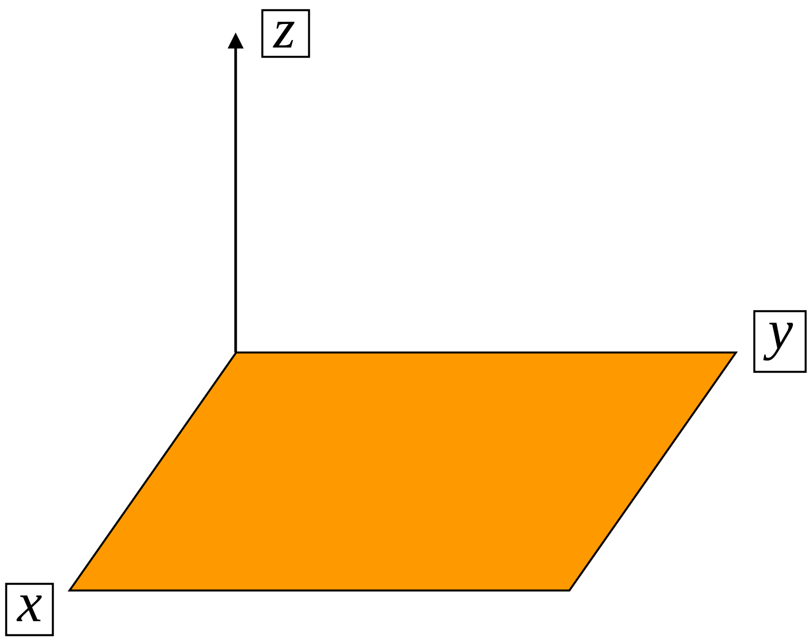

Department of Physics and Astronomy
Georgia State University
Atlanta, GA 30303-3083

Maxwell Equations in the absence of the external currents and charges:

$$\text{for } \mathbf{E}, \mathbf{H} \propto \exp(-i\omega t)$$

$$\nabla \times \mathbf{E} = -\frac{1}{c}\frac{\partial \mathbf{B}}{\partial t} \quad \Rightarrow \quad \nabla \times \mathbf{E} = i k_0 \mu \mathbf{H}$$

$$\nabla \times \mathbf{H} = \frac{1}{c}\frac{\partial \mathbf{D}}{\partial t} \quad \Rightarrow \quad \nabla \times \mathbf{H} = -i k_0 \varepsilon \mathbf{E}, \quad \text{where } k_0 \equiv \frac{\omega}{c}$$

$$\nabla \mathbf{D} = 0 \ ,$$

$$\nabla \mathbf{H} = 0 \, ; \quad \mathbf{F} = e\mathbf{E} + \frac{e}{c}[\mathbf{v} \times \mathbf{B}] \quad \text{Lorentz formuala}$$

See, e.g., L. D. Landau and E. M. Lifshitz, *Electrodynamics of Continuous Media* (Pergamon, Oxford and New York, 1984).

Department of Physics and Astronomy
Georgia State University
Atlanta, GA 30303-3083

General type of linear response

$$\mathbf{D}(\mathbf{r},t)=\int_{-\infty}^{\infty}\varepsilon(\mathbf{r}-\mathbf{r}',t-t')\mathbf{E}(\mathbf{r}',t')dt'd^3r'$$

$$\mathbf{B}(\mathbf{r},t)=\int_{-\infty}^{\infty}\mu(\mathbf{r}-\mathbf{r}',t-t')\mathbf{H}(\mathbf{r}',t')dt'd^3r'$$

Local response

$$\mathbf{D}(\mathbf{r},t)=\int_{-\infty}^{\infty}\varepsilon(\mathbf{r},t-t')\mathbf{E}(\mathbf{r},t')dt' \quad\Rightarrow\quad \mathbf{D}(\omega)=\varepsilon(\omega)\mathbf{E}(\omega)$$

$$\mathbf{B}(\mathbf{r},t)=\int_{-\infty}^{\infty}\mu(\mathbf{r},t-t')\mathbf{H}(\mathbf{r},t')dt' \quad\Rightarrow\quad \mathbf{B}(\omega)=\mu(\omega)\mathbf{H}(\omega)$$

$$\mathbf{D}(\omega)=\int_{-\infty}^{\infty}\mathbf{D}(t)e^{i\omega t}dt,\quad \mathbf{D}(t)=\int_{-\infty}^{\infty}\mathbf{D}(\omega)e^{-i\omega t}\frac{d\omega}{2\pi},$$

Relation between permittivity and conductivity (Optional)

$$\text{Continuity eq.}: \frac{\partial \rho(t)}{\partial t} + \frac{\partial \mathbf{j}(t)}{\partial \mathbf{r}} = 0 \quad \Rightarrow$$

$$\rho = -\frac{\partial \mathbf{P}}{\partial \mathbf{r}} \quad \Rightarrow \qquad \mathbf{j}(t) = \frac{\partial \mathbf{P}(t)}{\partial t} \quad \Rightarrow \mathbf{j}(\omega) = -i\omega \mathbf{P}(\omega)$$

$$\mathbf{D}(\omega) = \mathbf{E}(\omega) + 4\pi \mathbf{P}(\omega) = \varepsilon(\omega)\mathbf{E}(\omega) \quad \Rightarrow \mathbf{P}(\omega) = \frac{\varepsilon(\omega) - 1}{4\pi}\mathbf{E}(\omega)$$

$$\mathbf{j}(\omega) = -i\omega \frac{\varepsilon(\omega) - 1}{4\pi}\mathbf{E}(\omega)$$

$$\mathbf{j}(\omega) = \sigma(\omega)\mathbf{E}(\omega) \qquad \Rightarrow \boxed{\begin{aligned} \sigma(\omega) &= -i\omega \frac{\varepsilon(\omega) - 1}{4\pi} \\ \varepsilon(\omega) &= 1 + i\frac{4\pi}{\omega}\sigma(\omega) \end{aligned}}$$

Seeking for solution as a TM wave

(To be confirmed by equations)

$$\mathbf{H} = \left(H_x(y,z,t),0,0\right)$$
$$\mathbf{E} = \left(0, E_y(y,z,t), E_z(y,z,t)\right)$$

Spatio-temporal dependence:

$$H_x(y,z,t) = H_x(z)\exp\left(iky - i\omega t\right)$$
$$E_i(y,z,t) = E_i(z)\exp\left(iky - i\omega t\right),\ i = y, z$$

Wave equations are obtained by applying curl operation to Maxwell equations:

$$\left(\nabla^2 + k_0^2\varepsilon\mu\right)\mathbf{H} = 0 \quad \Rightarrow \quad \left(\frac{\partial^2}{\partial z^2} - k^2 + k_0^2\varepsilon\mu\right)H_x = 0$$

$$\left(\nabla^2 + k_0^2\varepsilon\mu\right)\mathbf{E} = 0 \quad \Rightarrow \quad \left(\frac{\partial^2}{\partial z^2} - k^2 + k_0^2\varepsilon\mu\right)E_{y,z} = 0$$

Department of Physics and Astronomy
Georgia State University
Atlanta, GA 30303-3083

Seeking $$H_x(z) \propto \exp(\pm\kappa z), \quad E_{y,z}(z) \propto \exp(\pm\kappa z)$$

From the wave equations: $k_0^2\varepsilon\mu = k^2 - \kappa^2, \quad k_0 = \dfrac{\omega}{c};$

$$\nabla \times \mathbf{H} = -ik_0\varepsilon\mathbf{E} \quad \Rightarrow$$

$$x: \quad \frac{\partial H_z}{\partial y} - \frac{\partial H_y}{\partial z} = -ik_0\varepsilon E_x \quad \Rightarrow \quad E_x = 0$$

$$y: \quad \frac{\partial H_x}{\partial z} - \frac{\partial H_z}{\partial x} = -ik_0\varepsilon E_y \quad \Rightarrow \quad E_y = \pm\frac{i\kappa}{k_0\varepsilon}H_x$$

$$z: \quad \frac{\partial H_y}{\partial x} - \frac{\partial H_x}{\partial y} = -ik_0\varepsilon E_z \quad \Rightarrow \quad E_z = \frac{k}{k_0\varepsilon}H_x$$

Because we have already satisfied the wave equations, the second Maxwell equations is the satisfied identically

Boundary conditions are continuity across the interface plane of

$$H_x \quad \text{and} \quad E_y = \frac{i}{k_0\varepsilon}\frac{\partial H_x}{\partial z}$$

Surface plasmon polariton (SPP) in a planar layered medium is a TM wave where in an *i*-th medium layer at a point (*y, z)* for a wave propagating in the *y* direction

$$H_x(i,y,z) = \left[A_i \exp(\kappa_i z) + B_i \exp(-\kappa_i z)\right]\exp(iky),$$

$$E_y(i,y,z) = \frac{i\kappa_i}{\varepsilon_i k_0}\left[A_i \exp(\kappa_i z) - B_i \exp(-\kappa_i z)\right]\exp(iky),$$

$$E_z(i,y,z) = \frac{k}{\varepsilon_i} H_x(i,y,z);$$

$$k \equiv k_y; \quad k_0^2\varepsilon\mu = k^2 - \kappa^2, \quad k_0 = \frac{\omega}{c}; \; i = 1,2,\ldots \text{is layer number}$$

Department of Physics and Astronomy
Georgia State University
Atlanta, GA 30303-3083

Boundary conditions :

$$H_x(1,y,z) = H_x(2,y,z)$$

$$E_y(1,y,z) = E_y(2,y,z)$$

These conditions reduce to :

$$B_1 = A_2$$

$$\frac{\kappa_1}{\varepsilon_1} = -\frac{\kappa_2}{\varepsilon_2}$$

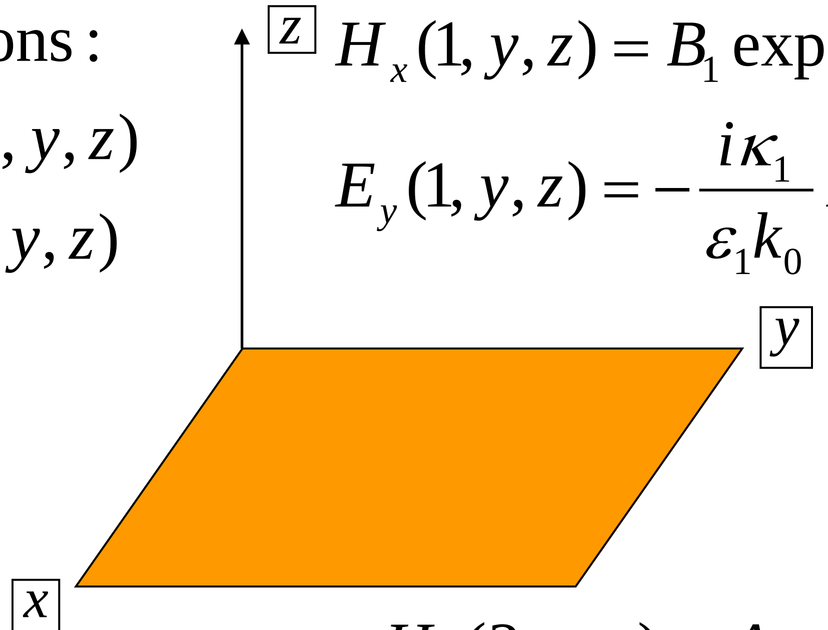

$$H_x(1,y,z) = B_1 \exp(-\kappa_1 z)\exp(iky),$$

$$E_y(1,y,z) = -\frac{i\kappa_1}{\varepsilon_1 k_0} B_1 \exp(-\kappa_i z)\exp(iky),$$

$$H_x(2,y,z) = A_2 \exp(\kappa_2 z)\exp(iky),$$

$$E_y(2,y,z) = \frac{i\kappa_2}{\varepsilon_2 k_0} A_2 \exp(\kappa_2 z)\exp(iky).$$

Boundary conditions:

$$\frac{\kappa_1}{\varepsilon_1}=-\frac{\kappa_2}{\varepsilon_2}$$

Wave equations:

$$k_0^2\varepsilon_1=k^2-\kappa_1^2$$

$$k_0^2\varepsilon_2=k^2-\kappa_2^2$$

Definition:

$$k_0=\frac{\omega}{c}$$

Transforming:

$$\frac{\kappa_1^2}{\varepsilon_1^2}=\frac{\kappa_2^2}{\varepsilon_2^2} \quad \Rightarrow$$

Substituting: $\Downarrow$

$$\frac{k_0^2\varepsilon_1-k^2}{\varepsilon_1^2}=\frac{k_0^2\varepsilon_2-k^2}{\varepsilon_2^2}$$

Algebraically solving for k^2: $\quad k^2=k_0^2\dfrac{\varepsilon_1\varepsilon_2}{\varepsilon_1+\varepsilon_2}$

Finding by substitution: $\quad \kappa_1^2=-k_0^2\dfrac{\varepsilon_1^2}{\varepsilon_1+\varepsilon_2}, \quad \kappa_2^2=-k_0^2\dfrac{\varepsilon_2^2}{\varepsilon_1+\varepsilon_2}.$

Metal-Dielectric Interface

For a two-medium system, the SPP wave vector is found as a function of frequency (dispersion relation):

$$k = \frac{\omega}{c}\sqrt{\frac{\varepsilon_1\varepsilon_2}{\varepsilon_1+\varepsilon_2}}$$

Evanescent decay exponents in these two media are found as

$$\kappa_1 = \frac{\omega}{c}\sqrt{-\frac{\varepsilon_1^2}{\varepsilon_1+\varepsilon_2}} \qquad \kappa_2 = \frac{\omega}{c}\sqrt{-\frac{\varepsilon_2^2}{\varepsilon_1+\varepsilon_2}}$$

From these, it follows that for the existence of SPPs, it is necessary and sufficient that $\varepsilon_1+\varepsilon_2<0$ and $\varepsilon_1\varepsilon_2<0$

Dielectric permittivity for silver and gold in optical region

P. B. Johnson and R. W. Christy, "Optical-Constants of Noble-Metals," *Physical Review B* **6**, 4370-4379 (1972).

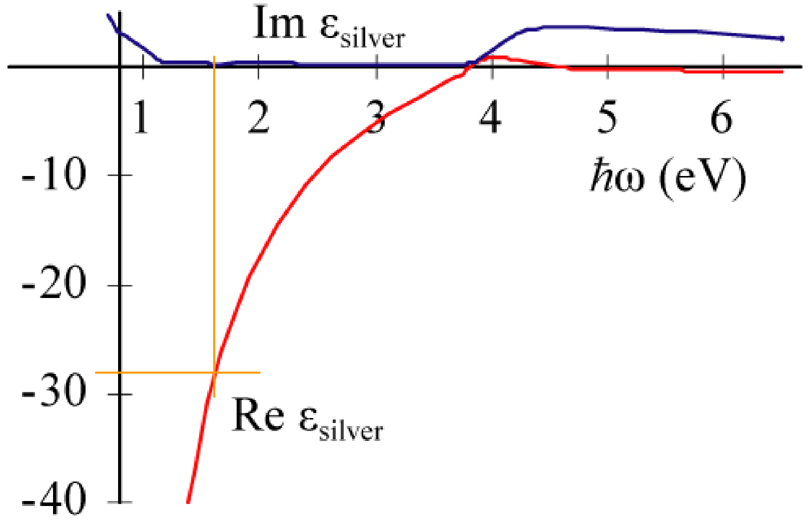

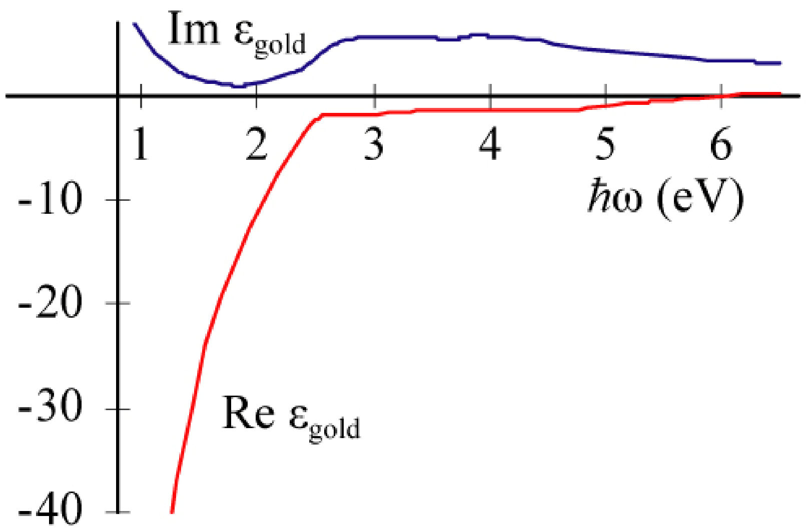

$$\lambda[\mu] = \frac{1.24}{\omega[\text{eV}]}$$

Drude formula: $\varepsilon = \varepsilon_0 - \dfrac{\omega_p^2}{\omega(\omega + i\gamma)}$

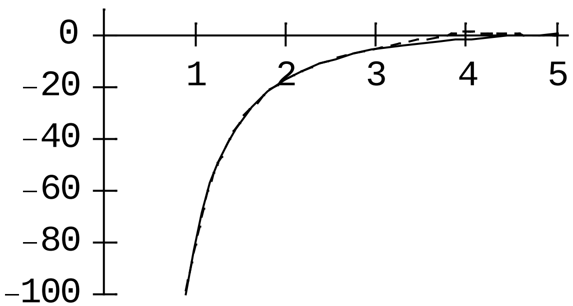

$\mathrm{Re}\,\varepsilon;\ \ \varepsilon_0 = 3.6; \omega_p = 9.1\ \text{eV}$

$\mathrm{Im}\,\varepsilon;\ \ \gamma = 0.02\ \text{eV}$

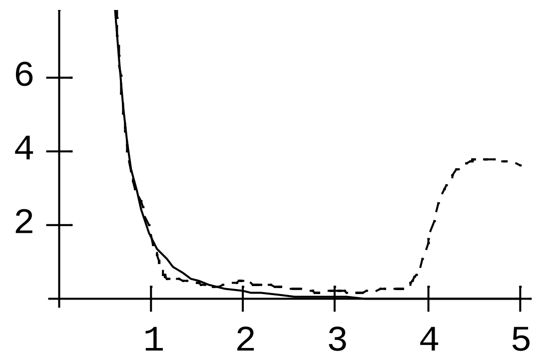

$\omega\,(\text{eV})$

Fit to near-ir

$\mathrm{Im}\,\varepsilon;\ \ \gamma = 0.055\ \text{eV}$

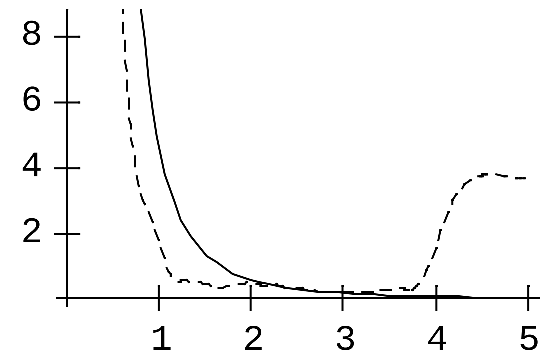

$\omega\,(\text{eV})$

Fit to visible

Department of Physics and Astronomy
Georgia State University
Atlanta, GA 30303-3083

Surface plasmon dispersion and resonance for real silver [data of Johnson and Christy, P. B. Johnson and R. W. Christy, *Optical-Constants of Noble-Metals*, Phys. Rev. B 6, 4370-4379 (1972)**]**

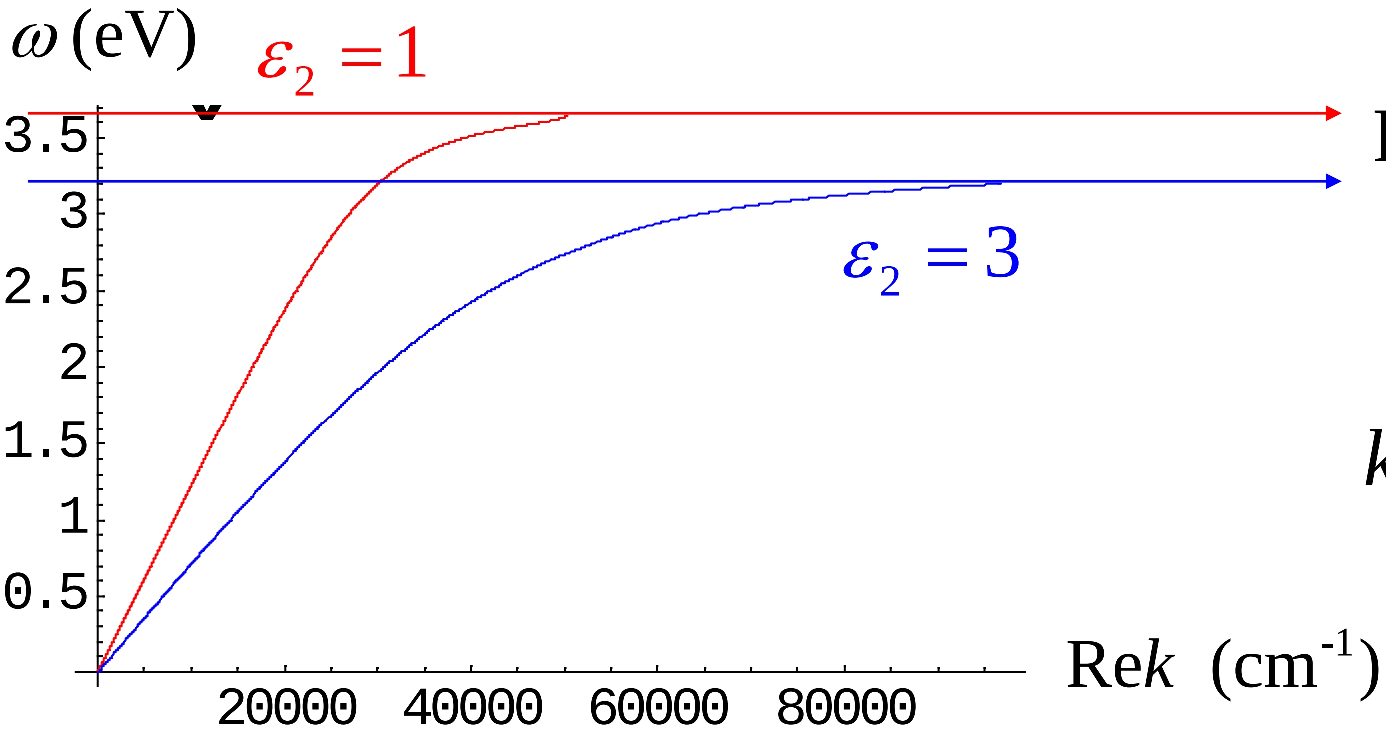

$$\mathrm{Re}[\varepsilon_1 + \varepsilon_2] = 0$$

$$k = \frac{\omega}{c}\sqrt{\frac{\varepsilon_1 \varepsilon_2}{\varepsilon_1 + \varepsilon_2}}$$

[Inverse wavelength in cm]

Department of Physics and Astronomy
Georgia State University
Atlanta, GA 30303-3083

Surface Plasmon Polaritons and Sommerfeld-Zenneck Waves (example for silver in vacuum)

$$k = \frac{\omega}{c}\sqrt{\frac{\varepsilon_m(\omega)}{\varepsilon_m(\omega)+1}} \qquad \kappa_{\text{vacuum}} = \frac{\omega}{c}\sqrt{-\frac{1}{\varepsilon_m(\omega)+1}}$$

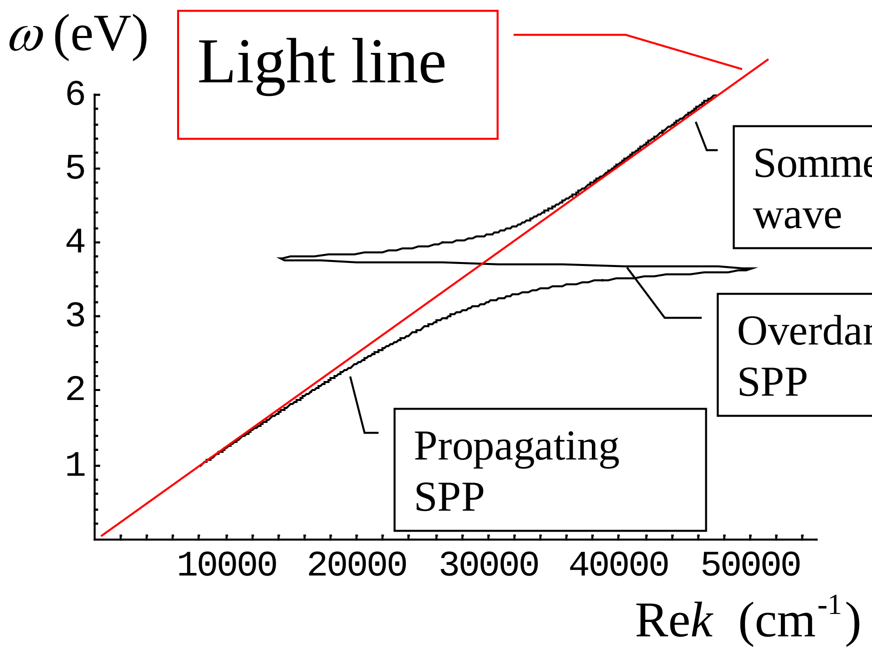

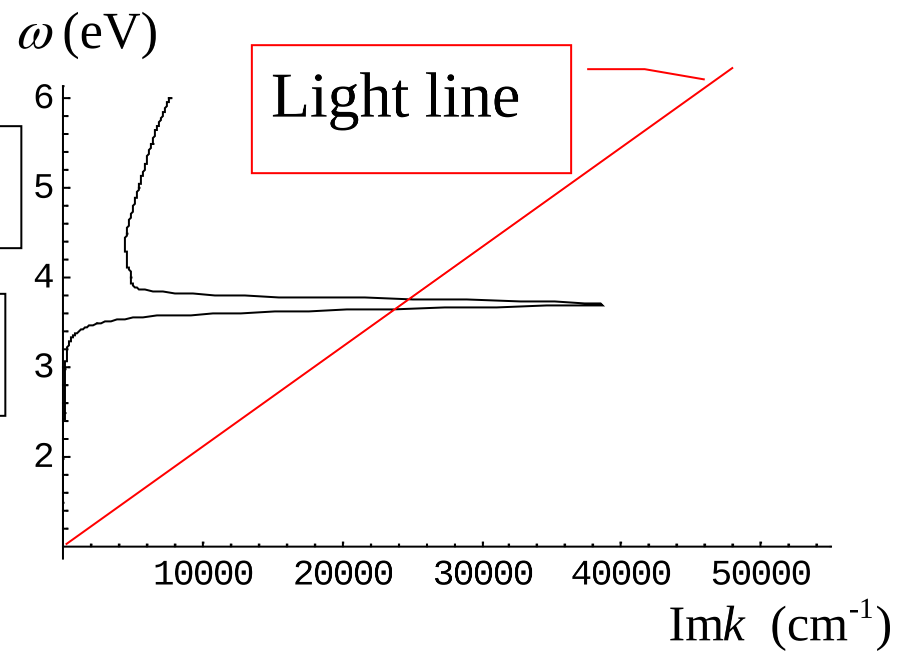

Surface plasmon polariton fields

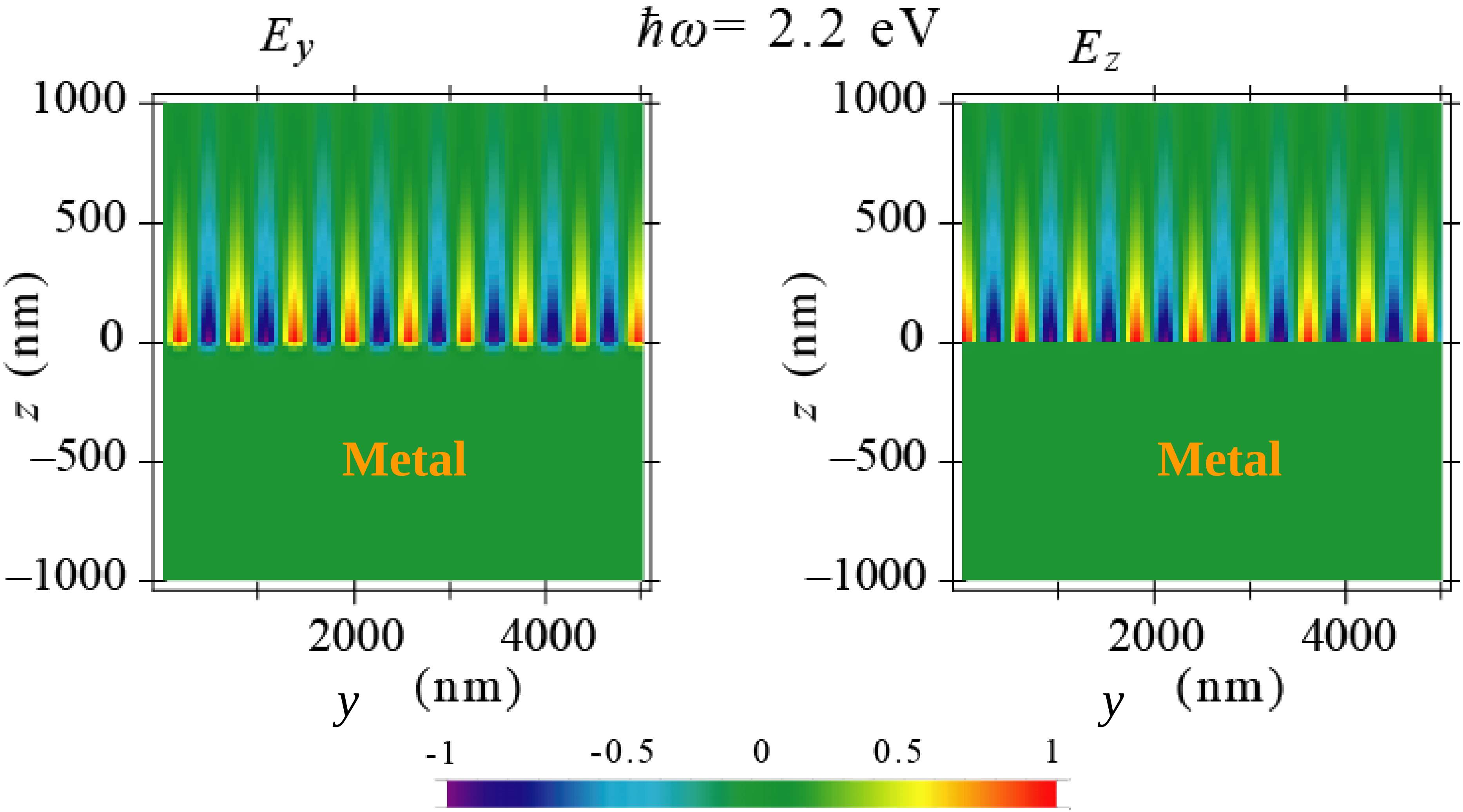

Surface plasmon polaritons fields

$\hbar\omega = 3.0$ eV

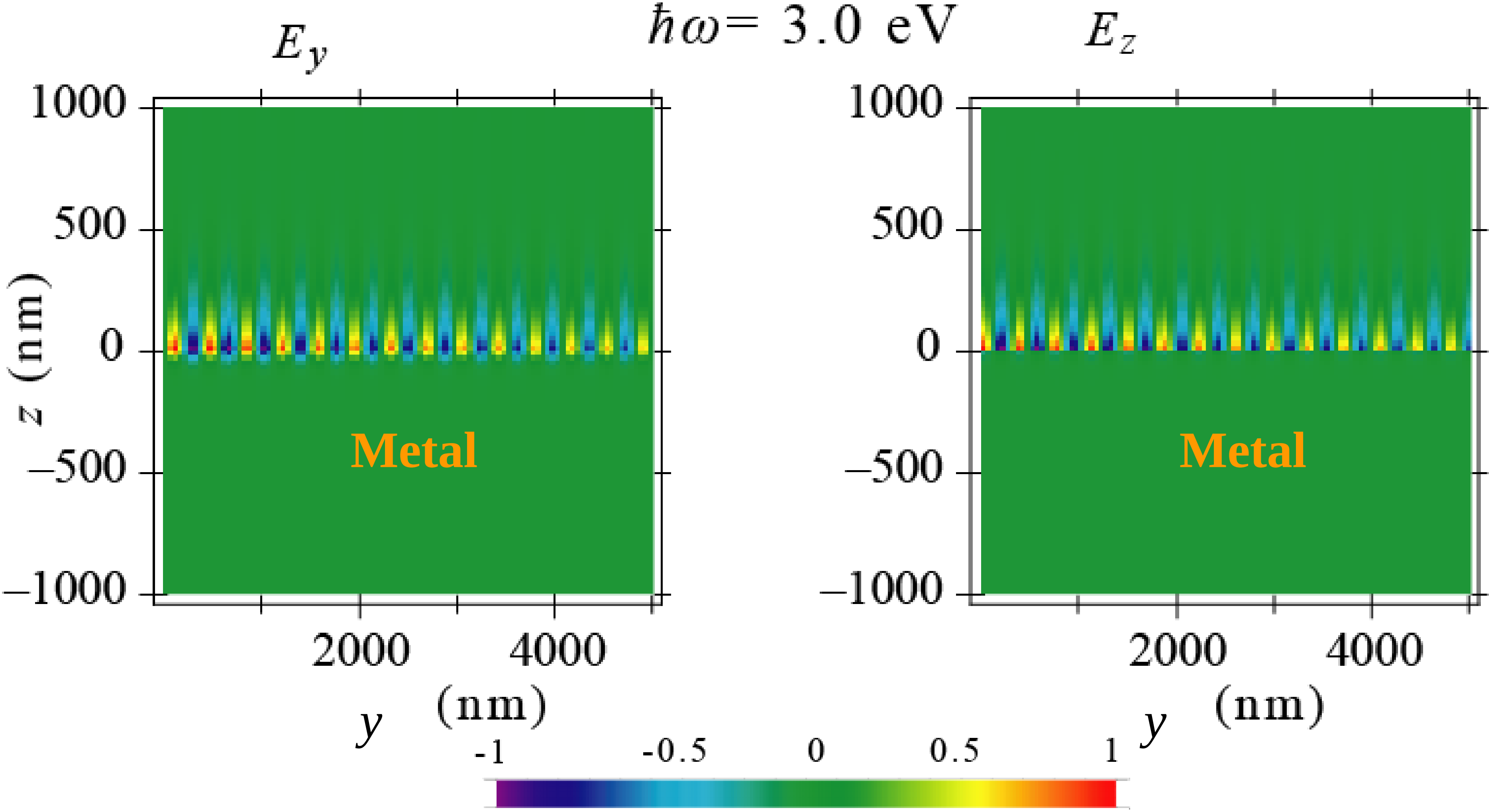

Topography of Surface Plasmon Polariton Electric Fields

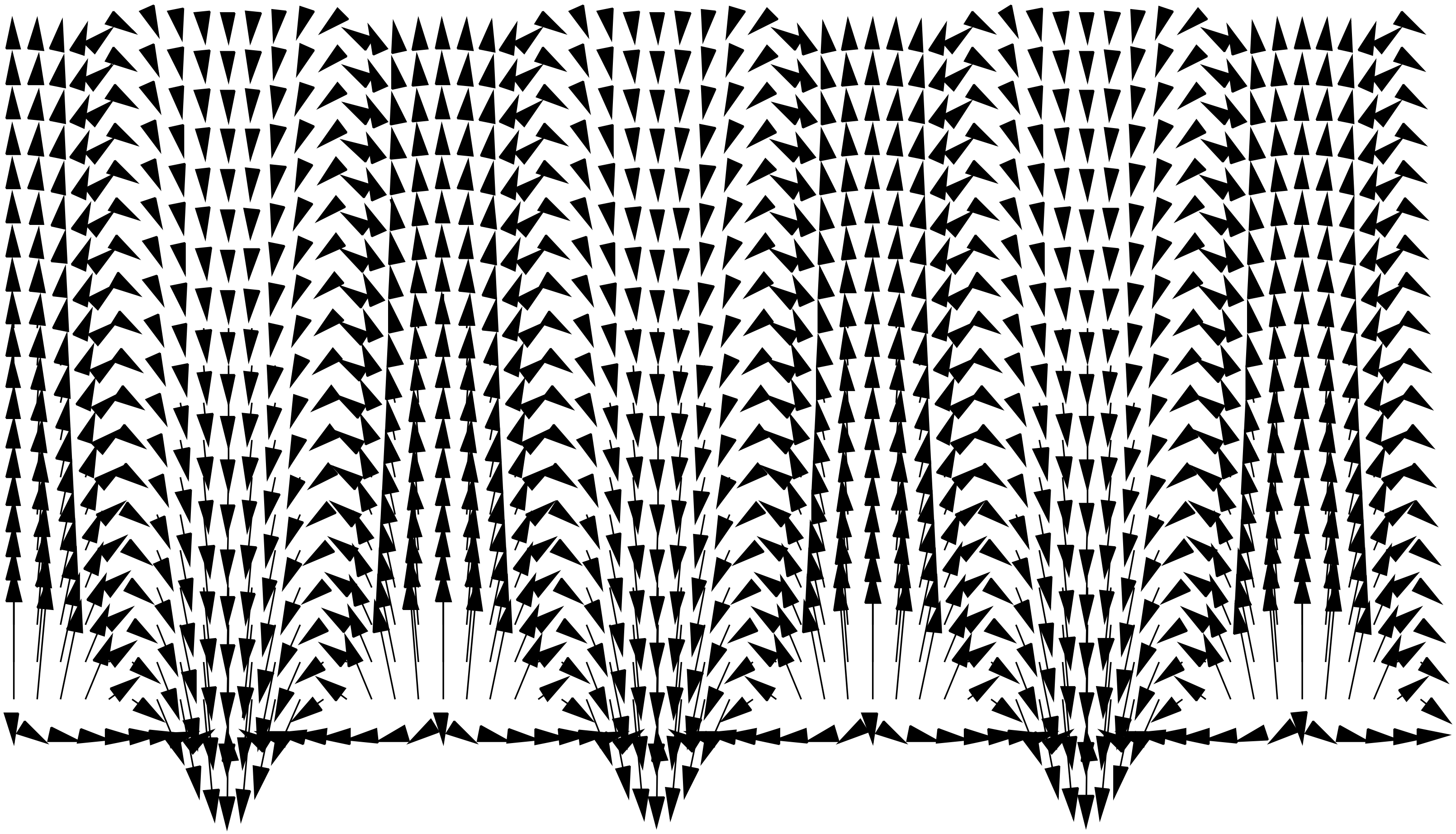

SPP excitation in Kretschmann geometry and SPP sensing

Sensors: http://www.biacore.com/

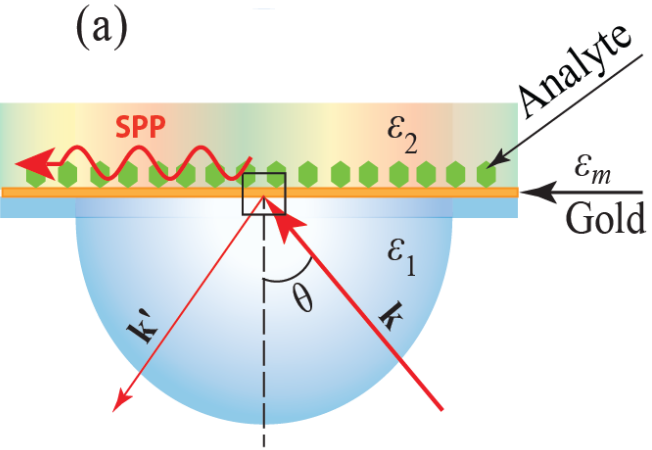

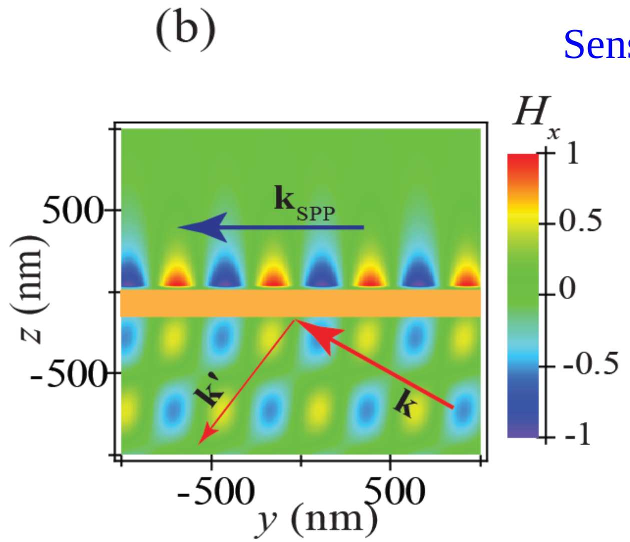

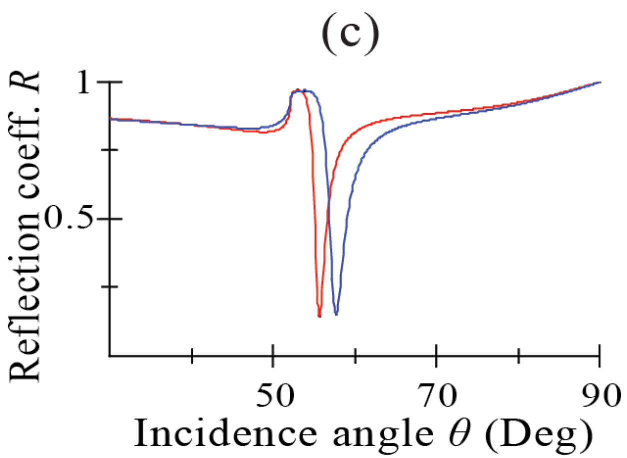

$$\sqrt{\varepsilon_1}\sin\theta_K = \sqrt{\frac{\varepsilon_m \varepsilon_2}{\varepsilon_m + \varepsilon_2}},$$ where θ_K is Kretschmann angle

$$\varepsilon_1 > \frac{\varepsilon_m \varepsilon_2}{\varepsilon_m + \varepsilon_2} > \varepsilon_2$$

$$\sqrt{\varepsilon_1}\sin\theta_{TIR} = \sqrt{\varepsilon_2},$$ where θ_{TIR} is total internal reflection angle

$$\theta_K > \theta_{TIR}$$

Three-Layer Systems

Dispersion relation (exact analytical expression), where *d* is the layer thickness: defines the SPP wave vector *k*

$$\exp\left[2k_0 d\varepsilon_2 u_2\right]=\frac{\left(u_1-u_2\right)\times\left(u_3-u_2\right)}{\left(u_1+u_2\right)\times\left(u_3+u_2\right)};\quad u_i=\frac{1}{\varepsilon_i}\sqrt{\frac{k^2}{k_0^2}-\varepsilon_i};\quad k_0=\frac{\omega}{c}$$

Here ε_i is dielectric premittivity of i-th layer

Another form:

$$\tanh\left[k_0 d\varepsilon_2 u_2\right]=-\frac{u_2\left(u_1+u_3\right)}{u_1u_3+u_2^2}$$

Fast SPP root
(Long range SPP)

Slow SPP root
(Short range SPP)

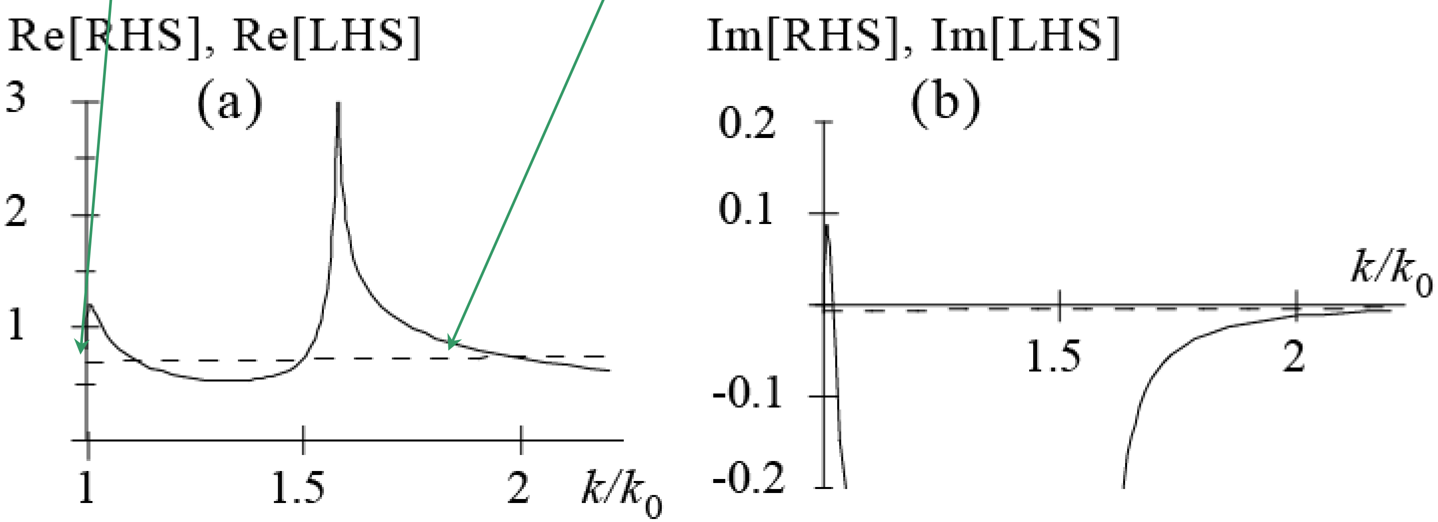

Two roots for nano-thin silver in vacuum: Symmetric and Antisymmetric SPPs. No cut-off for SPP as thickness tends to zero

Dispersion Relations for Symmetric Systems

$$\varepsilon_1 = \varepsilon_3$$

$$\tanh\left[k_0 d \varepsilon_2 u_2\right] + \frac{2u_1 u_2}{u_1^2 + u_2^2} = 0$$

Parity (symmetry) is conventionally defined as that of the *normal (z)* component of the electric field or the magnetic field (*x*-component)

Even (symmetric) mode

$$\tanh\left[\frac{1}{2} k_0 d \varepsilon_2 u_2\right] = -\frac{u_1}{u_2}$$

Odd (antisymmetric) mode

$$\tanh\left[\frac{1}{2} k_0 d \varepsilon_2 u_2\right] = -\frac{u_2}{u_1}$$

Dispersion relations for nanofilm of silver in vacuum (IMI structure): Symmetric mode (dashed) and antisymmetric mode (solid line)

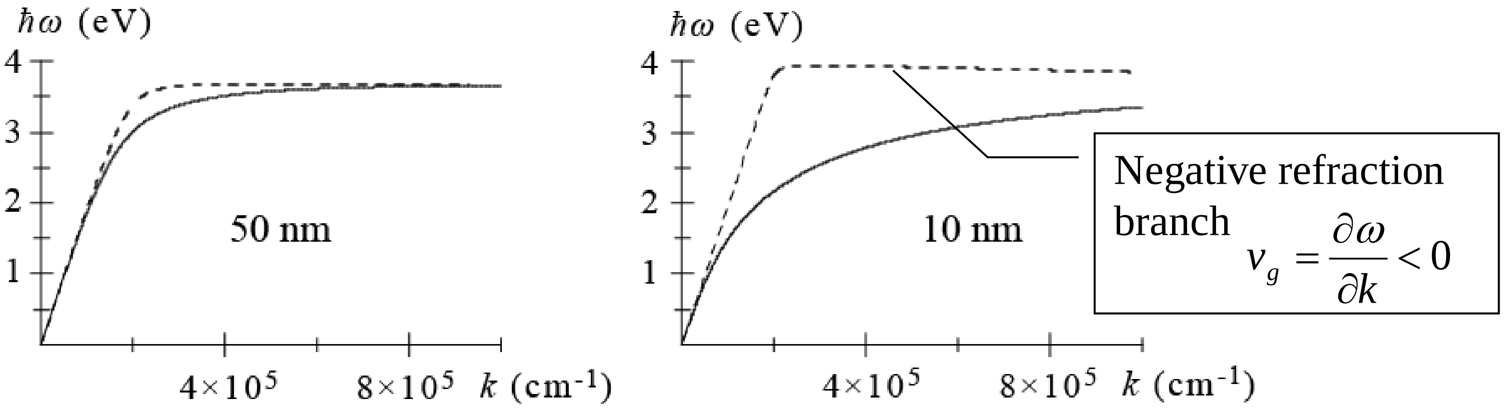

Decay exponent (Imk) for 30 nm silver layer

Symmetric mode

Antisymmetric mode

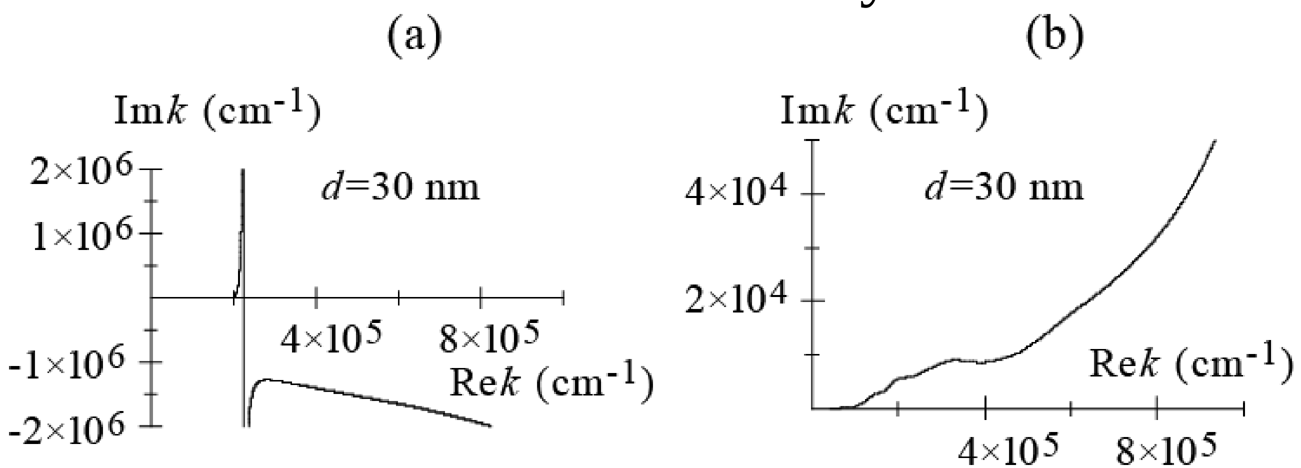

Local electric fields for 10 nm silver layer in vacuum at 2.2 eV frequency

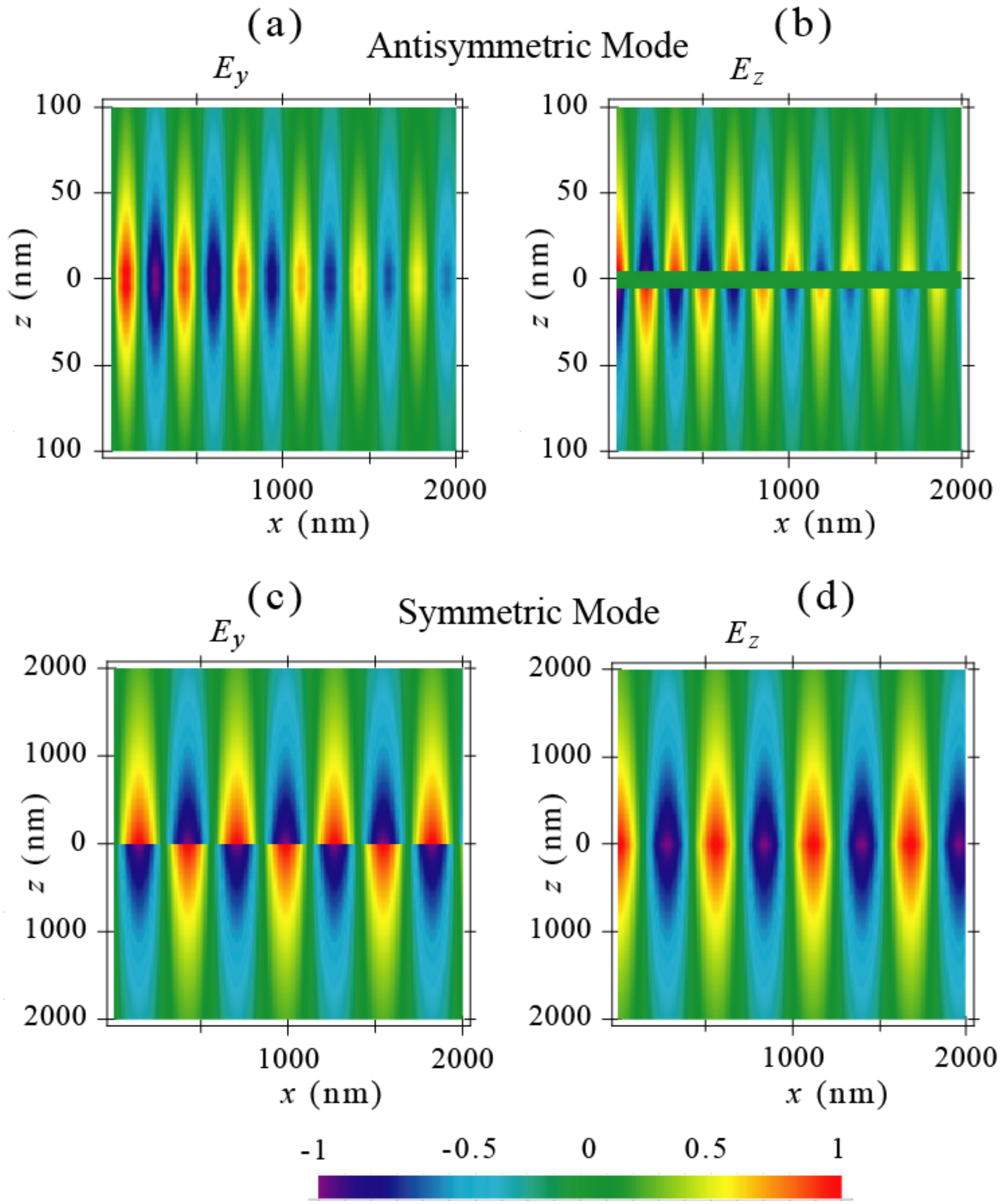

Georgia State University
Department of Physics and Astronomy
Georgia State University
Atlanta, GA 30303-3083

Local fields for 10 nm layer of silver in vacuum for a high wave vector

Rek=5 10^5 cm^{-1}

Antisymmetric mode: positive refraction

Symmetric mode: negative refraction, high loss (practically, no propagation).

The sign of refraction is determined by the sign of the group velocity $v_g = \partial\omega / \partial k$

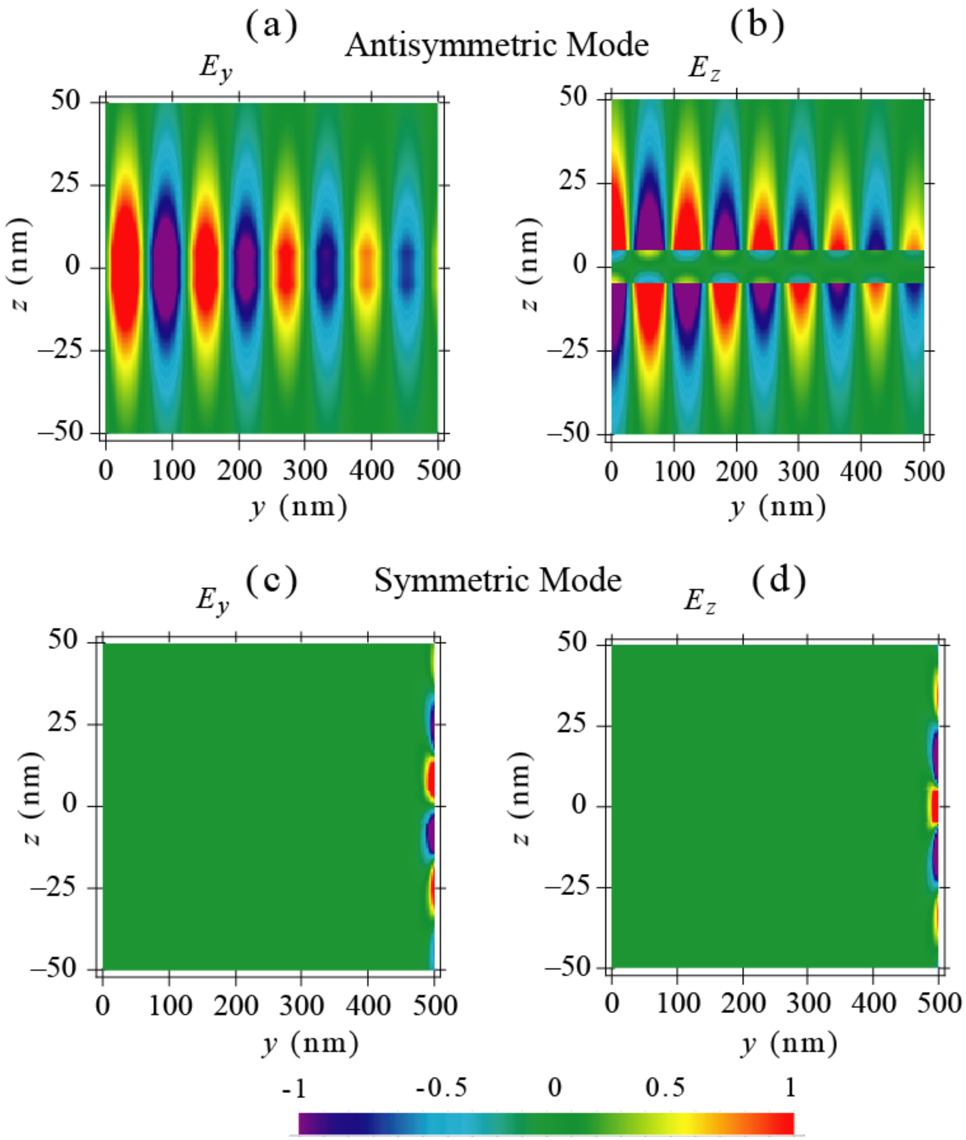

Department of Physics and Astronomy
Georgia State University
Atlanta, GA 30303-3083

SPPs in Dielectric Films (MIM)

$\varepsilon_m(\omega)$

ε_d

$\varepsilon_m(\omega)$

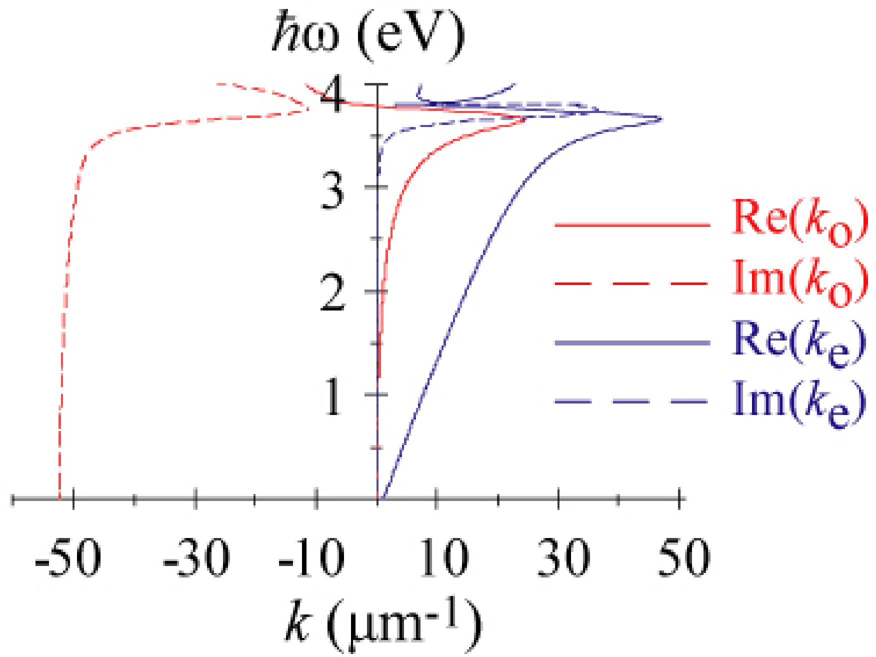

for **odd (antisymmetric) mode**: $\mathrm{Im}\, k_o \cdot \mathrm{Re}\, k_o < 0$ ⇨ negative refraction

for **all modes**: $\mathrm{Re}\, k_o \leq \left|\mathrm{Im}\, k_o\right|$ ⇨ large dissipation

Department of Physics and Astronomy
Georgia State University
Atlanta, GA 30303-3083

Radiative condition (other "causality"): Selecting one of the two solutions in electrodynamics. Mandelstam-Veselago's negative refraction

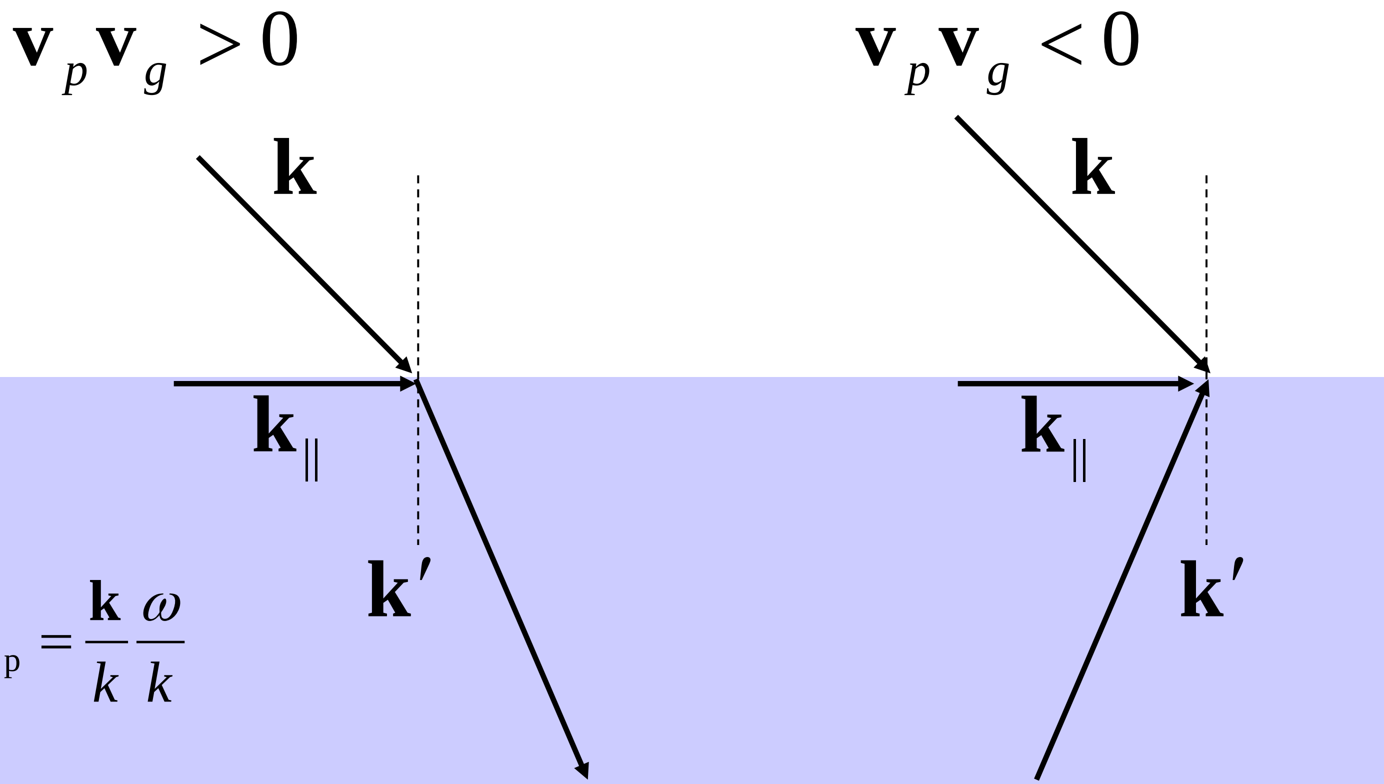

$$\mathbf{v}_{\mathrm{g}} = \frac{\mathbf{k}}{k}\frac{\partial \omega}{\partial k}; \quad \mathbf{v}_{\mathrm{p}} = \frac{\mathbf{k}}{k}\frac{\omega}{k}$$

Universal negative refraction condition from causality : $\mathrm{Im}\,\mathbf{k} \cdot \mathrm{Re}\,\mathbf{k} < 0$

Department of Physics and Astronomy
Georgia State University
Atlanta, GA 30303-3083

REPORTS

Negative Refraction at Visible Frequencies

20 APRIL 2007 VOL 316 SCIENCE

Henri J. Lezec,[1,2]*† Jennifer A. Dionne,[1]* Harry A. Atwater[1]

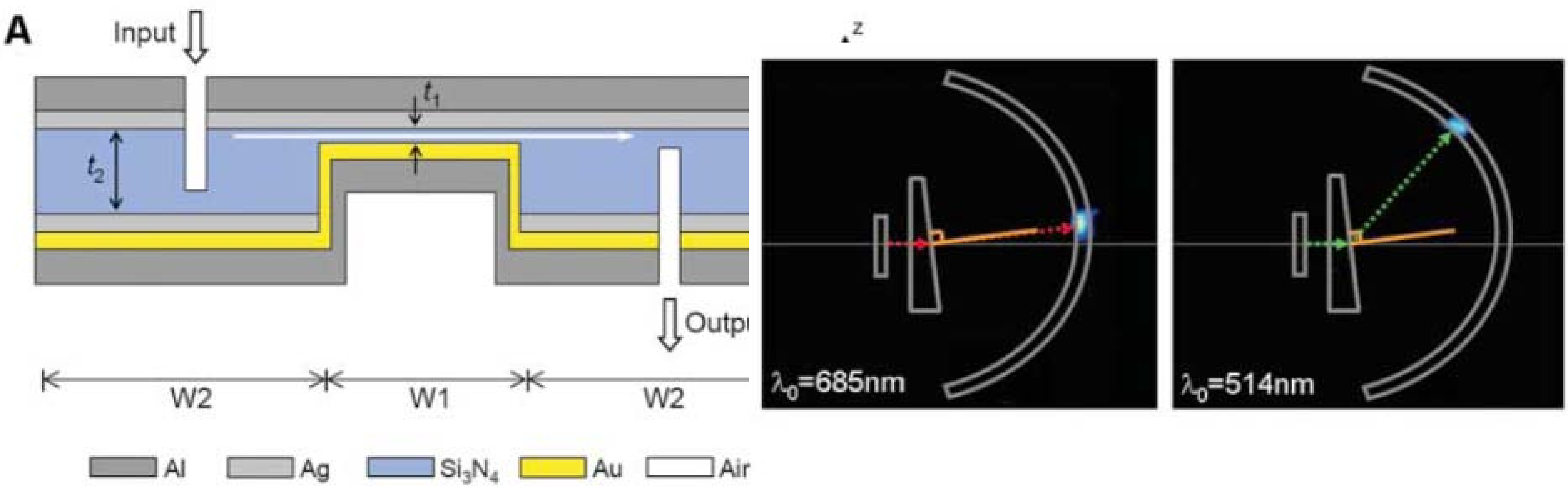

Criterion for Negative Refraction with Low Optical Losses from a Fundamental Principle of Causality

Mark I. Stockman*

General condition of negative refraction in isotropic medium (does not depend on choice of the square root sign for *n*):

$$\operatorname{Im} n^2 < 0 \quad \text{or} \quad \operatorname{Im} n \cdot \operatorname{Re} n < 0 \quad \text{or} \quad \operatorname{Im} \mathbf{k} \cdot \operatorname{Re} \mathbf{k} < 0;$$

$$\operatorname{Im} n^2 \equiv \operatorname{Re}\varepsilon \operatorname{Im}\mu + \operatorname{Re}\mu \operatorname{Im}\varepsilon.$$

Group velocity is the transfer of energy velocity only if loses are small enough.

If losses at the observation frequency are zero, then an exact causality relation is valid for isotropic medium without spatial dispersion:

$$\frac{c^2}{\mathbf{v}_p \mathbf{v}_g} = 1 + \frac{2}{\pi}\int_0^\infty \frac{\operatorname{Im} n^2(\omega_1)}{\left(\omega_1^2 - \omega^2\right)^2} d\omega_1 \text{, where } \omega \text{ is the observation frequency}$$

Criterion of negative refraction without loss at the observation frequency is

$$\int_0^\infty \frac{\operatorname{Im} n^2(\omega_1)}{\left(\omega_1^2 - \omega^2\right)^2} d\omega_1 < -\frac{\pi}{2}$$

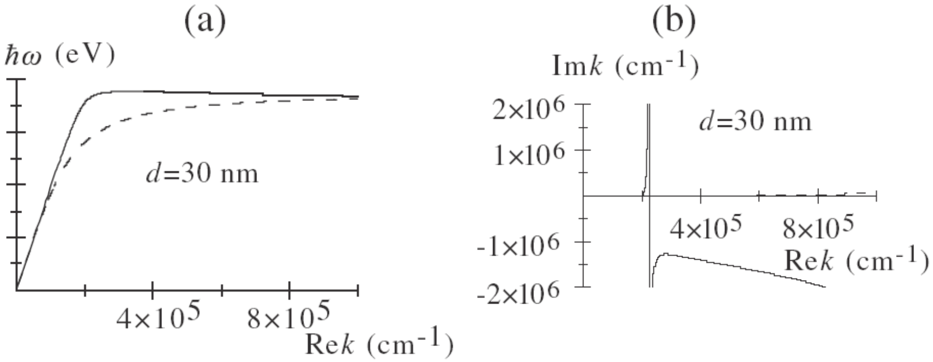

my

FIG. 1. Dispersion relations for thin silver film in vacuum. The symmetric and antisymmetric modes are displayed with solid and dashed lines, respectively. (a) Real part of dispersion relation: frequency ω as a function of Rek. (b) Imaginary part of the dispersion relation: dependence of Imk on Rek. Thickness of the silver film is $d = 30$ nm.

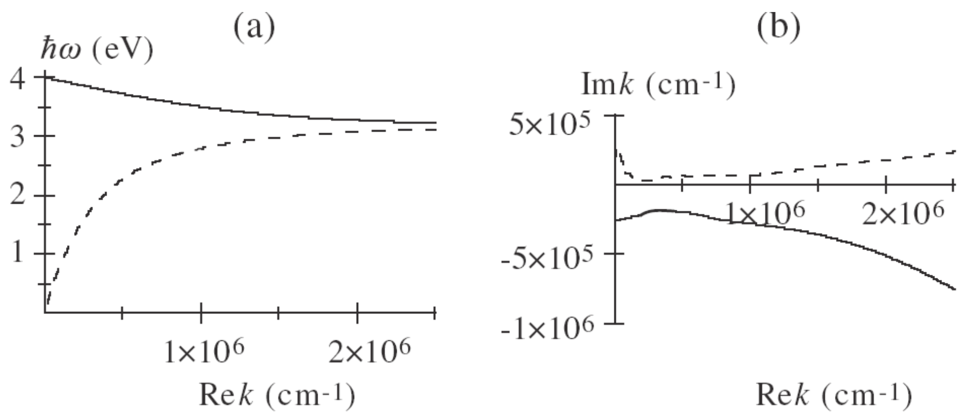

FIG. 2. (a) For a thin ($d = 10$ nm) dielectric layer with $\varepsilon_d = 3$ embedded in silver, dispersion relation of SPPs is displayed of as dependence of frequency $\hbar\omega$ on the real part of wave vector. (b) For the same system, dependence of Imk on Rek. For both panels, the solid lines pertain to the antisymmetric SPP mode, and the dashed lines denote the symmetric SPP mode.

CONCLUSIONS

1. In metal/dielectric layered systems there exist surface plasmon polariton (SPP) modes of different symmetries
2. For a metal layer in a dielectric medium, there are two types of SPP: symmetric (fast or long-range) SPP and antisymmetric (slow or short-range) SPP
3. Slow SPP for a thin metal film is nanolocalized at the surface of the film. It is useful to couple nanosystems to laser sources.
4. There is no cut-off as SPP wavelength tends to infinity.
5. Losses of negative refraction (back-propagating SPP) are very large
6. To have negative refraction without loss at an observation frequency, there must be loss in the adjacent region of negative refraction

Adiabatic Nano-Optics

Conventional (non-adiabatic) conversion to the near zone (direct excitation of local, near-zone fields by far-zone radiation) is very energy-inefficient, though can generate high local fields.

Both aperture and aperturless methods lead to loss of the major fraction of energy. If one could focus optical radiation from the far zone to nanoscale region, then the problem of the energy-efficient excitation of the local fields would have been solved. However, it is commonly known that it is impossible

Is it? We show that this common wisdom is wrong.

Using *adiabatic* transformation, one can transfer energy from the far zone to near field without major losses, with a high efficiency, limited only by absorption in plasmonic waveguides.

Department of Physics and Astronomy
Georgia State University
Atlanta, GA 30303-3083

Surface plasmon polaritons -> Surface plasmons

$$k = \frac{\omega}{c}\sqrt{\frac{\varepsilon_m \varepsilon_h}{\varepsilon_m + \varepsilon_h}},$$

$$\varepsilon_m \leq \varepsilon_h$$

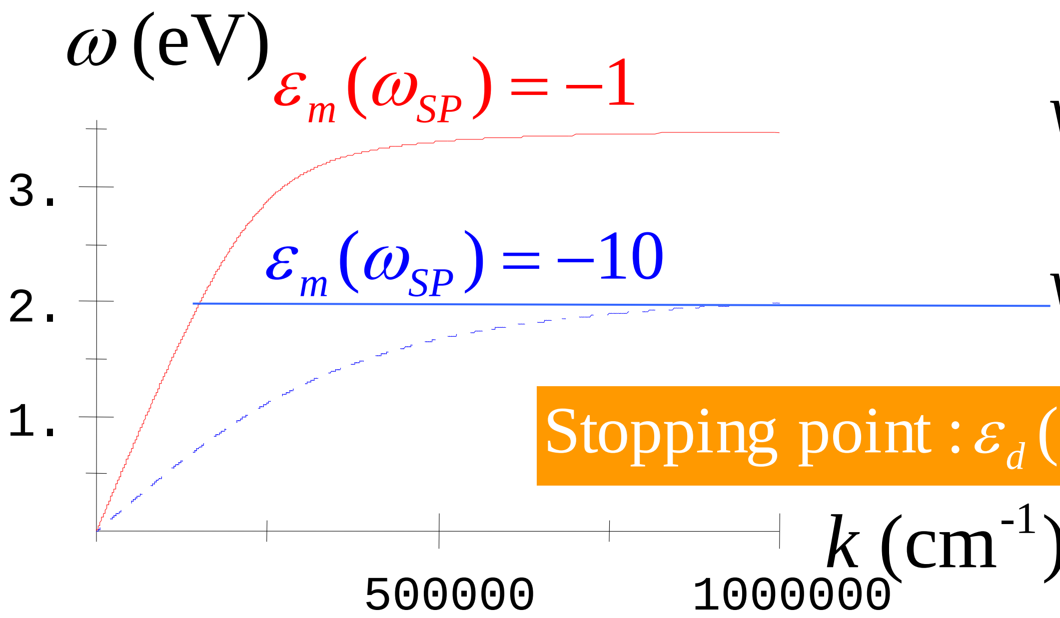

$$v_{phase} = \frac{\omega}{k} \to 0$$

$$v_{group} = \frac{d\omega}{dk} \to 0$$

Stopping point : $\varepsilon_d(z) = -\varepsilon_m(\omega)$

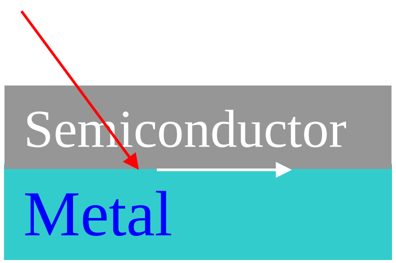

Department of Physic
Georgia State Univers
Atlanta, GA 30303-30

Adiabatic Slowing-Down and Stopping Surface Plasmon Polaritons

M. I. Stockman, in Plasmonics: Metallic Nanostructures and Their Optical Properties II, edited by N. J. Halas and T. R. Huser, *Delivering Energy to Nanoscale: Rapid Adiabatic Transformation, Concentration, and Stopping of Radiation in Nano-Optics* (SPIE, Denver, Colorado, 2004), Vol. 5512, p. 38-49

Dielectric function in the cross section of the system

$\lambda \approx 100$ nm

Graded semiconductor

Metal (Silver)

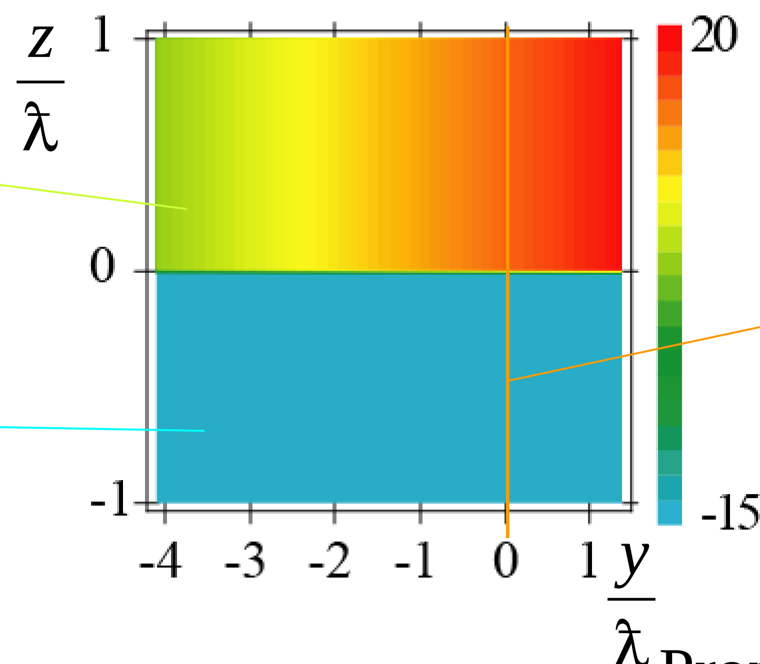

In the *x*-direction the system is uniform

Stopping point

$\varepsilon_d(z) = -\varepsilon_m(\omega)$

Propagation direction

Department of Physics and Ast
Georgia State University
Atlanta, GA 30303-3083

Adiabatic conversion in graded metal-semiconductor

Eikonal (WKB or quasiclassical) approximation is applicable because the grading is smooth (adiabatic)

Transverse electric field

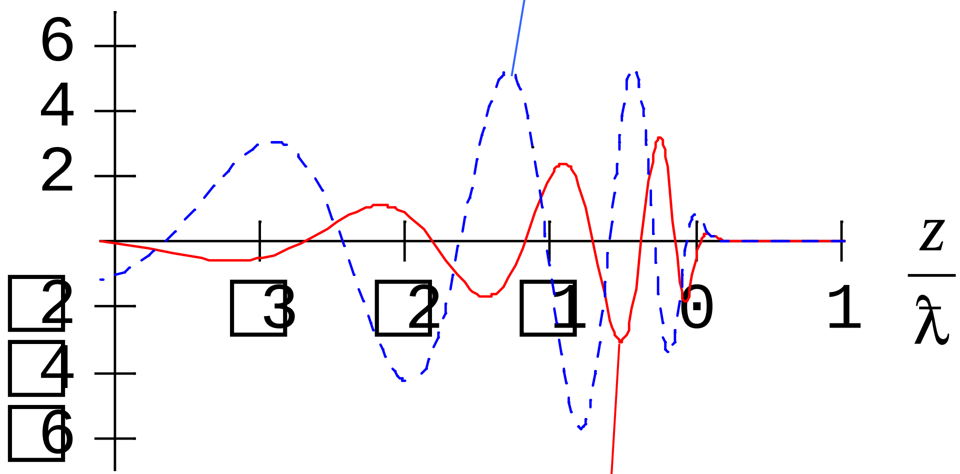

$\lambda \approx 100$ nm

Longitudinal electric field

→ Propagation direction

Department of Physics and Astronomy
Georgia State University
Atlanta, GA 30303-3083

Adiabatic Transformation and Accumulation of Local Fields in Graded Metal-Semiconductor Heterostructure

Intensity

$$I(\mathbf{r}) = \left|\mathbf{E}(\mathbf{r})\right|^2$$

Energy density

$$U(\mathbf{r}) = \frac{1}{8\pi}\left\{\frac{\partial\left[\omega\,\varepsilon(\mathbf{r},\omega)\right]}{\partial\omega}\left|\mathbf{E}(\mathbf{r})\right|^2 + \left|\mathbf{H}(\mathbf{r})\right|^2\right\}$$

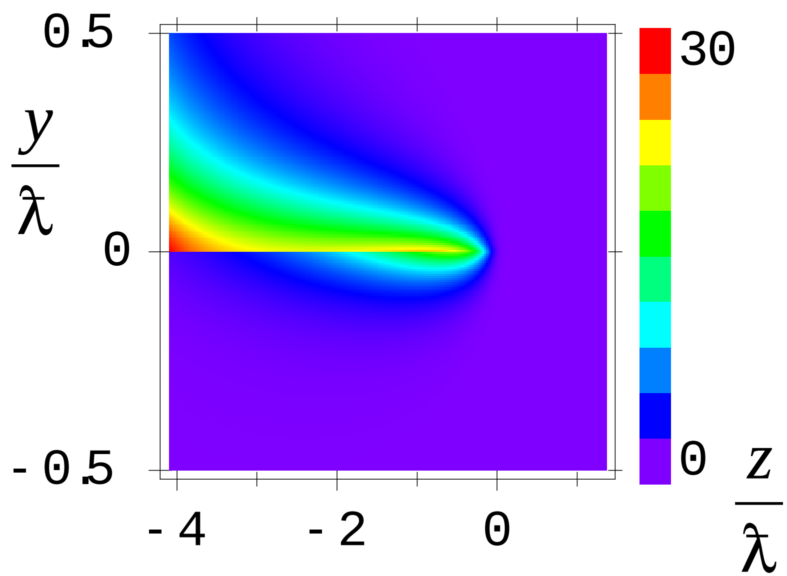

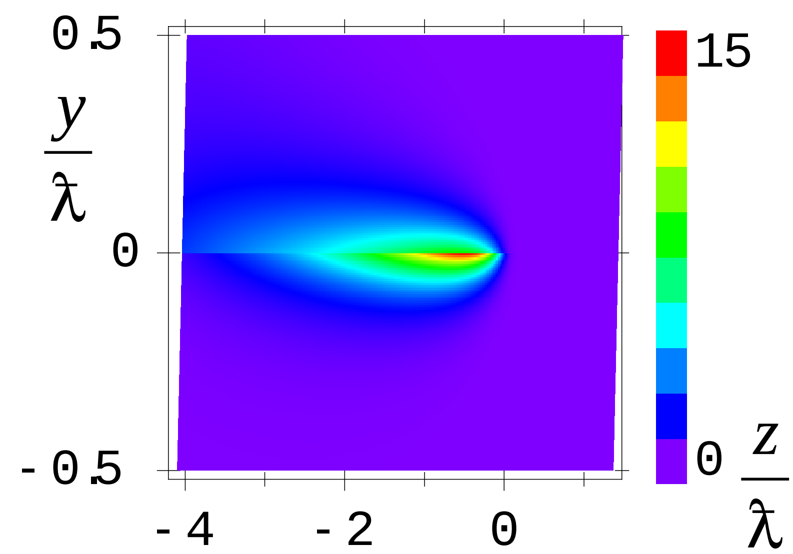

$\lambda \approx 100$ nm

Propagation direction

Department of Physics and Astronomy
Georgia State University
Atlanta, GA 30303-3083

Adiabatic Nanofocusing of Surface Plasmon Polaritons

M. I. Stockman, *Nanofocusing of Optical Energy in Tapered Plasmonic Waveguides*, Phys. Rev. Lett. **93**, 137404-1-4 (2004).

Waveguide geometry

Propagation direction

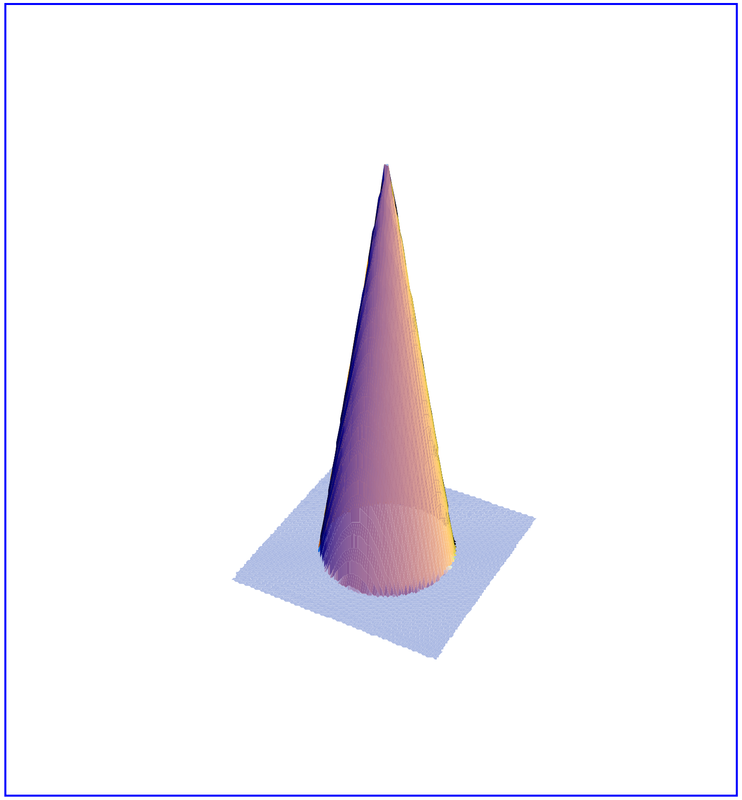

Department of Physics and Astronomy
Georgia State University
Atlanta, GA 30303-3083

For Cylindrical Plasmonic Waveguide

Electric field of SPP wave for TM_0 mode (magnetic field is tangential to the surface, normal to the axis; axially-symmetric solution)

$$r < R:\ E_z = I_0(\kappa_m r)\exp(ikz)$$

$$r > R:\ E_z = \frac{I_0(\kappa_m R)}{K_0(\kappa_d R)} K_0(\kappa_d r)\exp(ikz)$$

$$r < R:\ E_z = \frac{ik}{\kappa_m} I_1(\kappa_m r)\exp(ikz)$$

$$r > R:\ E_z = \frac{ik}{\kappa_d}\frac{I_0(\kappa_m R)}{K_0(\kappa_d R)} K_1(\kappa_d r)\exp(ikz)$$

Department of Physics and As
Georgia State University
Atlanta, GA 30303-3083

L. Novotny and C. Hafner, *Light Propagation in a Cylindrical Waveguide with a Complex, Metallic, Dielectric Function*, Phys. Rev. E **50**, 4094-4106 (1994)

For TM0 mode (magnetic field is tangential to the surface, normal to the axis; axially-symmetric solution), dispersion relation is

$$\frac{\varepsilon_m I_1(k_0 R\sqrt{k^2-\varepsilon_m})}{\sqrt{k^2-\varepsilon_m}\, I_0(k_0 R\sqrt{k^2-\varepsilon_m})} = -\frac{\varepsilon_d K_1(k_0 R\sqrt{k^2-\varepsilon_d})}{\sqrt{k^2-\varepsilon_d}\, K_0(k_0 R\sqrt{k^2-\varepsilon_d})}$$

$$k_0 = \frac{\omega}{c}$$

There is single root:

Slow SPP. There is no cutoff as its wavelength tends to zero (or wavevector tends to infinity)

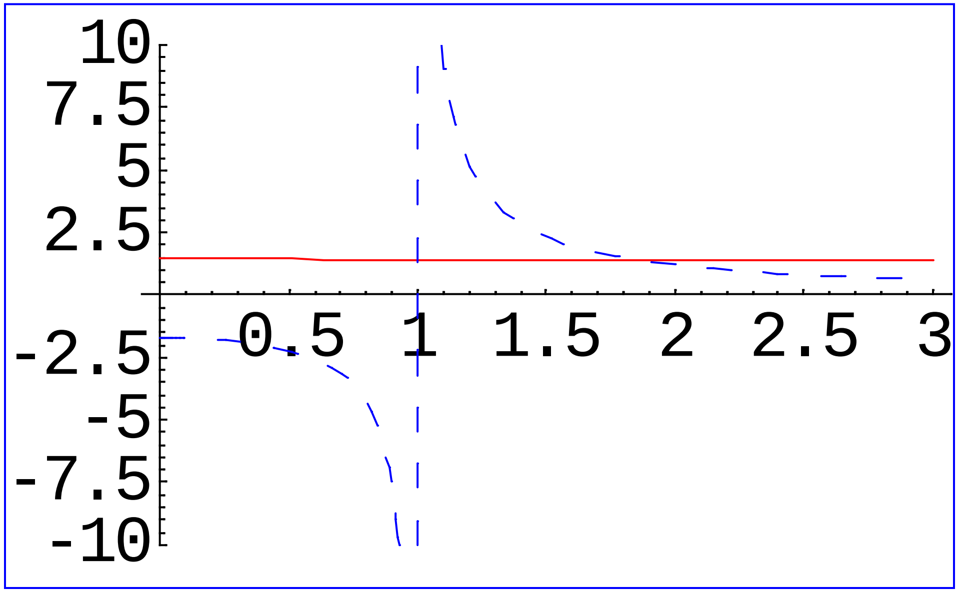

Introduce effective index: $k = n\omega/c$

Close to the tip ($R \longrightarrow 0$), this effective index diverges as 1/R:

$$n(R) \approx \frac{1}{k_0 R}\sqrt{\frac{2\varepsilon_d}{-\varepsilon_m}\frac{1}{\frac{1}{2}\log\frac{-4\varepsilon_m}{\varepsilon_d} - \gamma}}\ ,\ \gamma \approx 0.57721$$

This describes slowing down and asymptotic stopping of SPP. Important, the time to travel to the tip (singularity) of the conic waveguide logarithmically diverges,

$$t = \frac{1}{c}\int_{R_{\max}}^{R} n(r)dr \sim -\ln(k_0 R) \rightarrow \infty$$

Adiabatic parameter: $\delta = R' \dfrac{d\bar{\lambda}(R)}{dR}$

where $R' = \dfrac{dR(z)}{dz}$ is the waveguide grading

For a plasmonic (TM_0) mode, close to the tip

$$\delta \approx \left| R' \sqrt{-\frac{\varepsilon_m}{2\varepsilon_d}} \left[\ln \sqrt{-\frac{4\varepsilon_m}{\varepsilon_d}} - \gamma \right] \right|$$

Thus, adiabatic parameter stays finite everywhere, including the tip. Correspondingly, the adiabatic (eikonal or WKB) approximation is applicable uniformly over the entire tip.

Adiabatic Nanofocusing in Tapered Nanoplasmonic Waveguides

Intensity of Local Fields at the Surface of Tapered Plasmonic Waveguide (Conic Silver Wire)

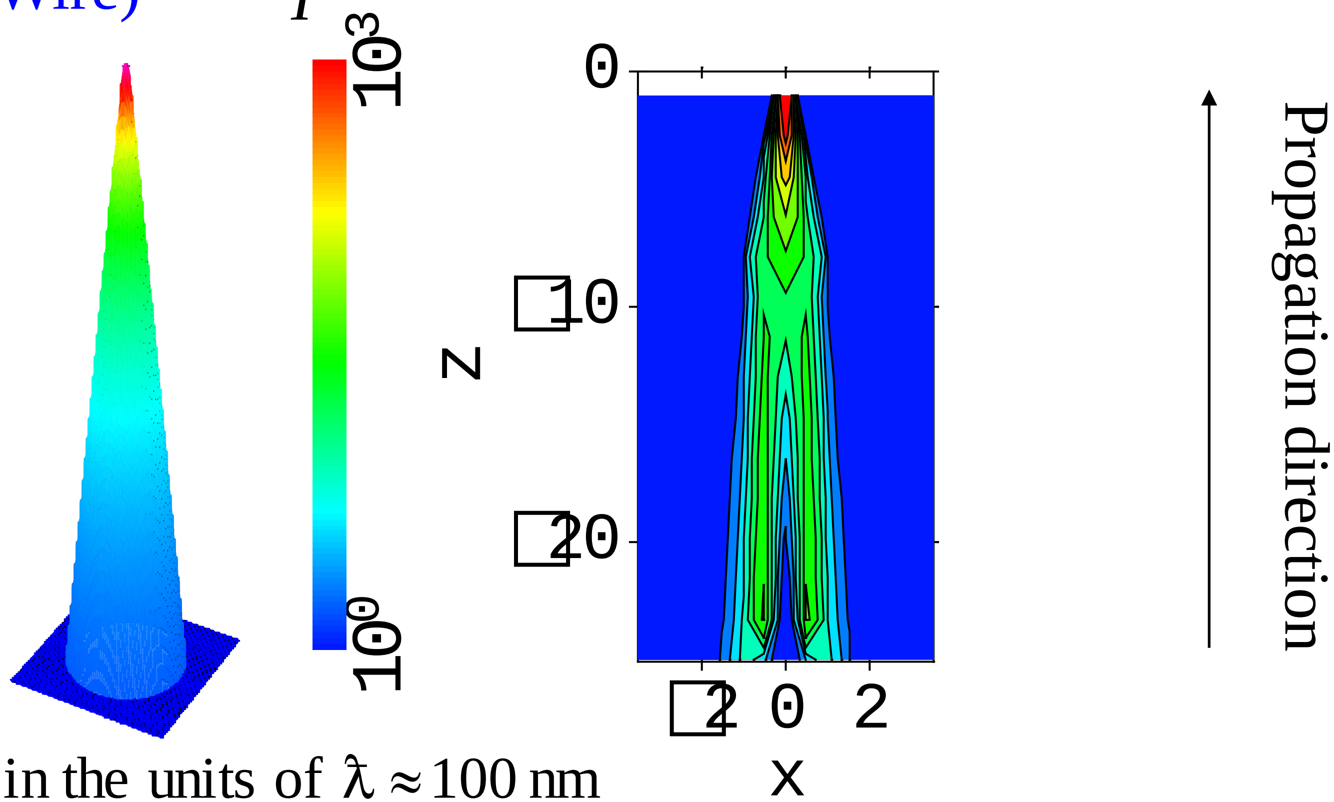

Coordinates are in the units of $\lambda\!\!\!^{-} \approx 100$ nm

M. I. Stockman, *Nanofocusing of Optical Energy in Tapered Plasmonic Waveguides*, Phys. Rev. Lett. **93**, 137404-1-4 (2004).

Department of Physics and Astronomy
Georgia State University
Atlanta, GA 30303-3083

Phase velocity of surface plasmon polaritons

Group velocity of surface plasmon polaritons

Adiabatic parameter (scaled by 10)

$$k(R) \approx \frac{1}{R}\sqrt{\frac{2\varepsilon_d}{-\varepsilon_m}\frac{1}{\frac{1}{2}\log\frac{-4\varepsilon_m}{\varepsilon_d}-\gamma}}$$

$$v_p = \left(\frac{k}{\omega}\right)^{-1} \propto R\,,\ v_g = \left(\frac{\partial k}{\partial \omega}\right)^{-1} \propto R$$

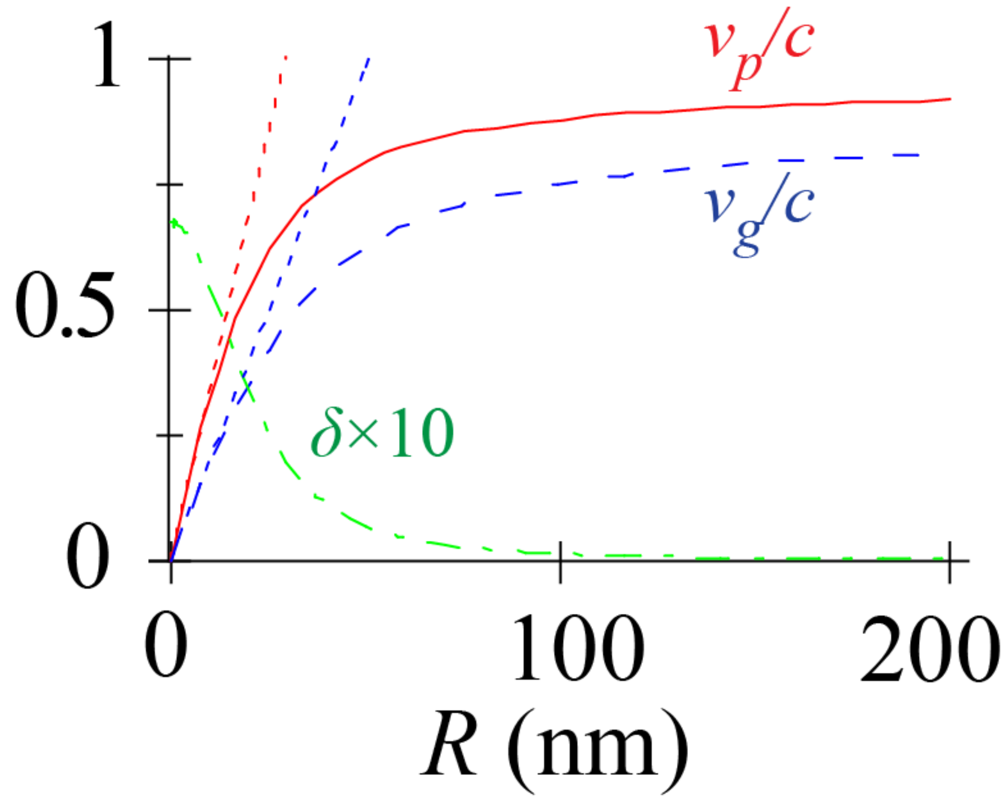

Department of Physics and Astronomy
Georgia State University
Atlanta, GA 30303-3083

Local Electric Fields at Surface of Plasmonic Tapered Waveguide

Transverse field

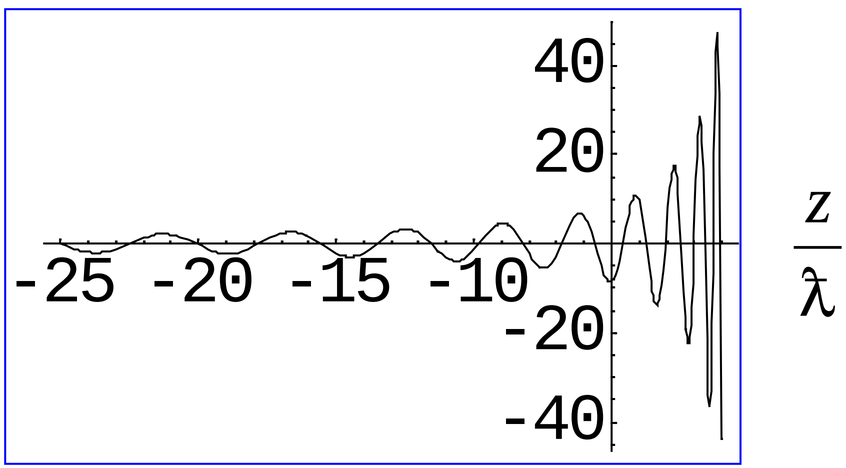

Longitudinal field

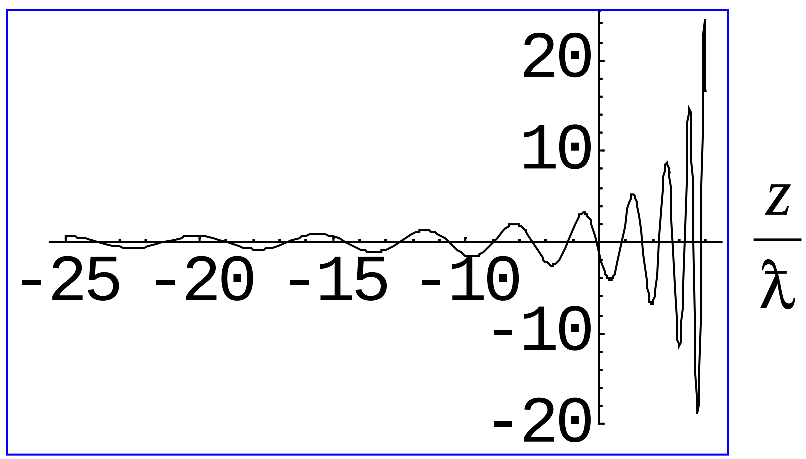

$\lambda \approx 100$ nm

Department of Physics and Astronomy
Georgia State University
Atlanta, GA 30303-3083

Local Electric Fields in Cross Section of System

Transverse electric field

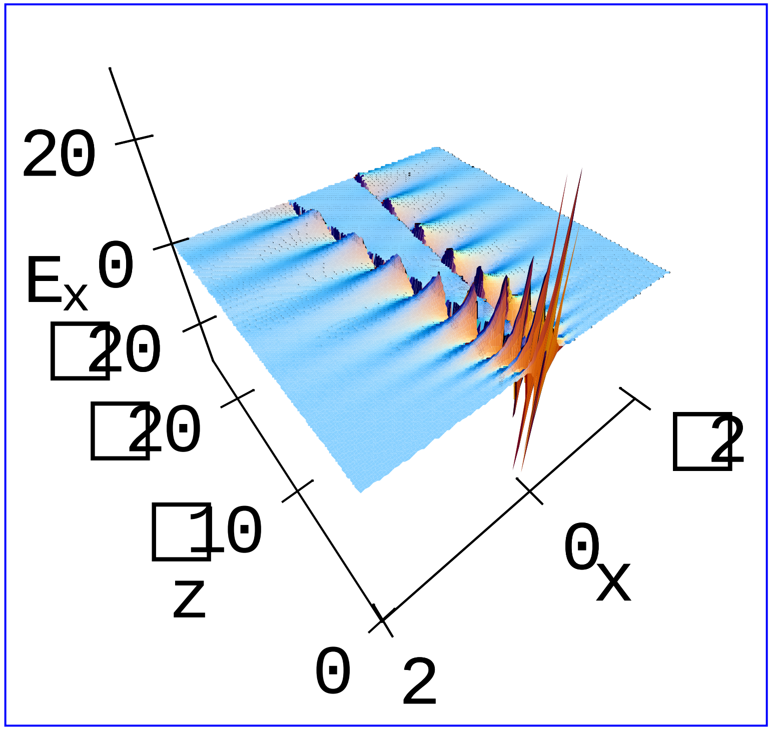

Longitudinal electric field

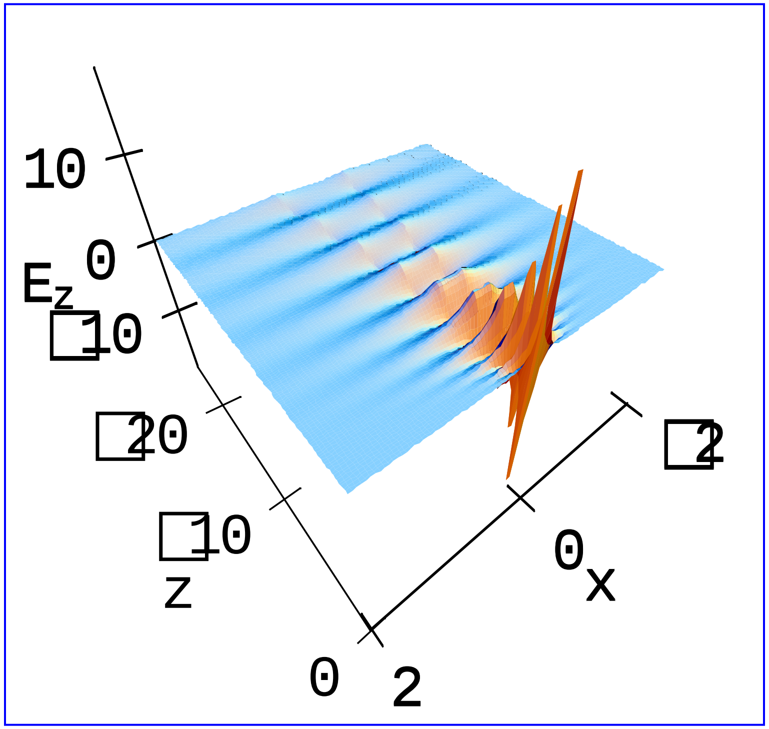

Coordinates are in the units of $\bar{\lambda} \approx 100$ nm

Vector of optical electric field for TM_0 plasmonic mode of conic waveguide made of silver

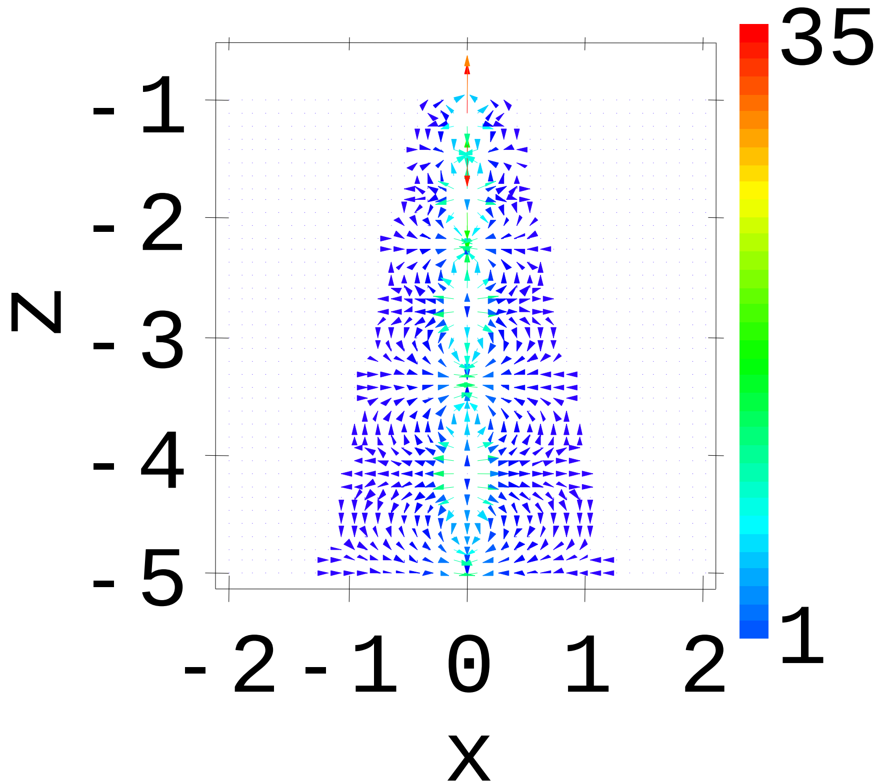

Spatial scales are in units of 100 nm

Department of Physics and Astronomy
Georgia State University
Atlanta, GA 30303-3083

Enhanced Nonlinear Optical Effects with a Tapered Plasmonic Waveguide

Ewold Verhagen,* Laurens Kuipers, and Albert Polman

Center for Nanophotonics, FOM Institute for Atomic and Molecular Physics (AMOLF), Kruislaan 407, 1098 SJ Amsterdam, The Netherlands

Nano Lett. **7**, 334-337 (2007)

(a)

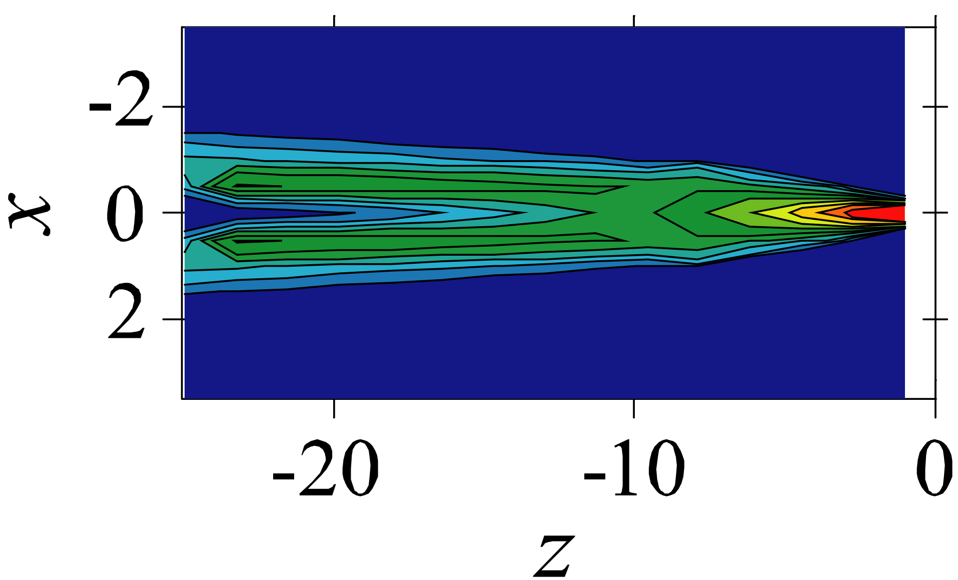

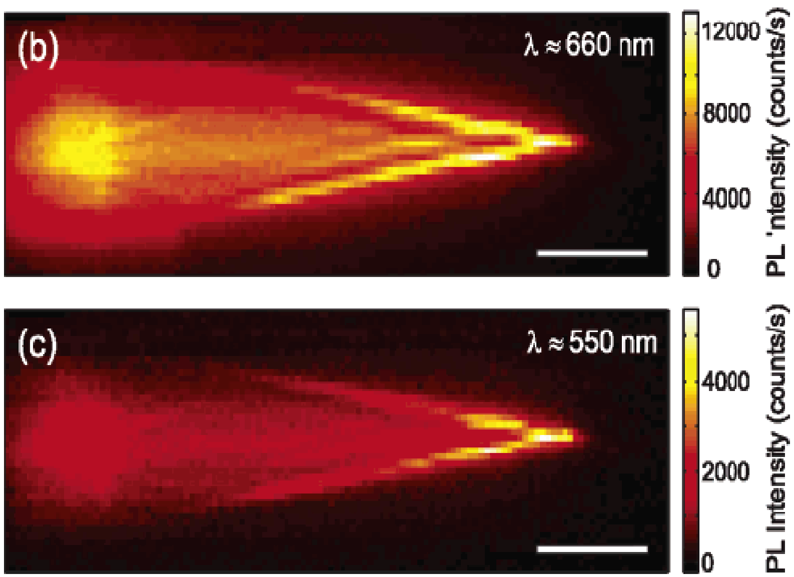

Department of Physics and Astronom
Georgia State University
Atlanta, GA 30303-3083

Latest: E. Verhagen, A. Polman, and L. Kuipers, *Nanofocusing in Laterally Tapered Plasmonic Waveguides*, Opt. Express **16**, 45-57 (2008)

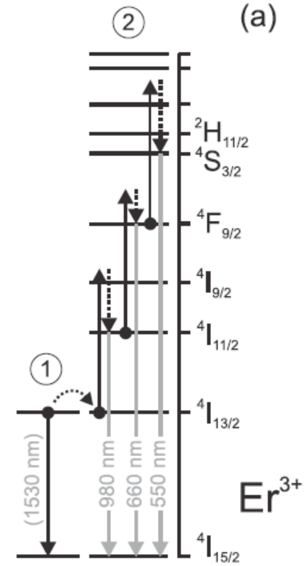

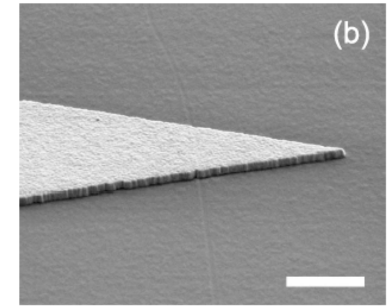

Fig. 1. (a) Energy level diagram of Er^{3+} ions. The black arrows depict the cooperative upconversion mechanism which causes the excitation of higher energy levels by energy
ge of the end of a fabricated, tapered Au
The scale bar is 1 μm.

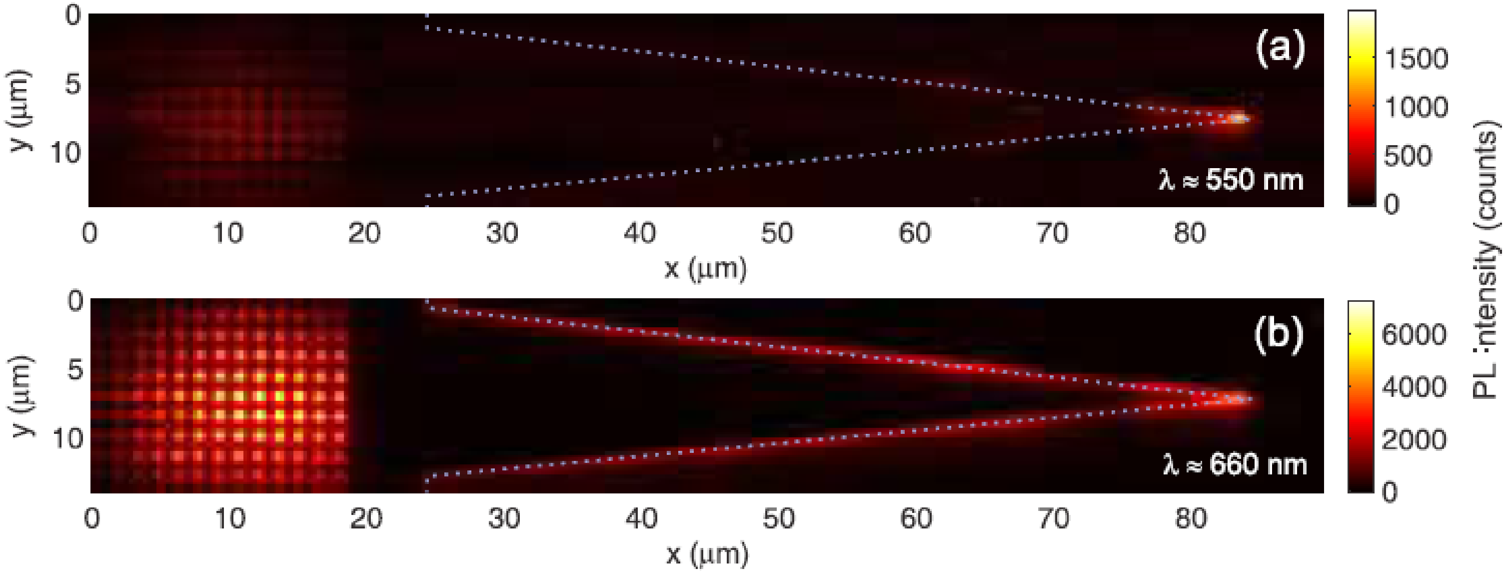

Fig. 5. Upconversion luminescence images taken from the air side of the film at (a) 550 nm and (b) 660 nm. The edge of the taper is indicated by the dotted line. Upconversion luminescence excited by SPPs on the substrate side of the film is observed from the edges of the taper, and the maximum intensity is detected at the taper tip.

PRL 102, 203904 (2009) PHYSICAL REVIEW LETTERS week ending 22 MAY 2009

Nanowire Plasmon Excitation by Adiabatic Mode Transformation

Ewold Verhagen,* Marko Spasenović, Albert Polman, and L. (Kobus) Kuipers
Center for Nanophotonics, FOM Institute for Atomic and Molecular Physics (AMOLF), Science Park 113, 1098 XG, Amsterdam, The Netherlands

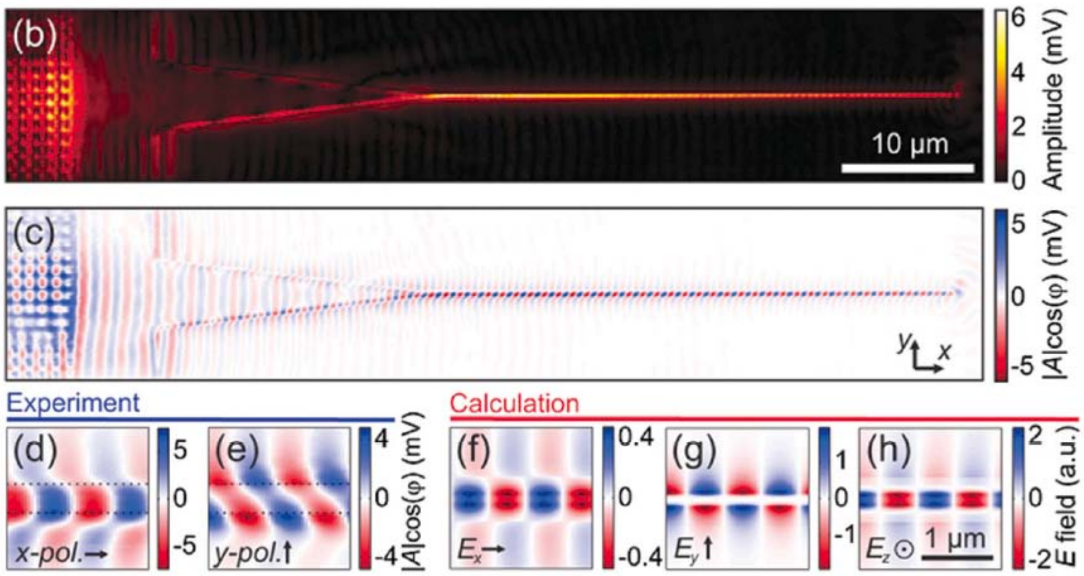

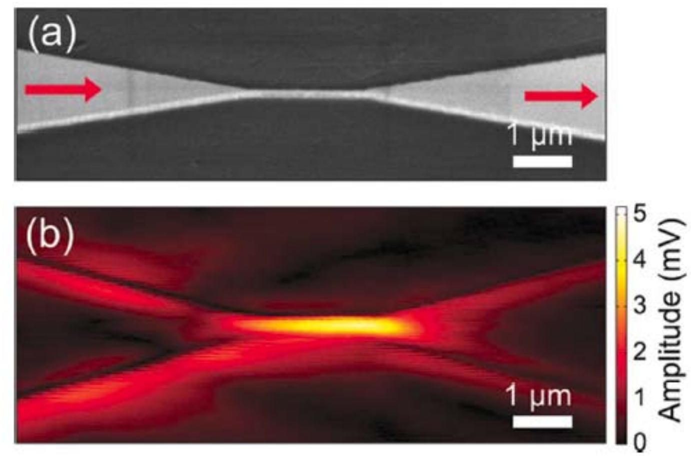

FIG. 4 (color). (a) Secondary electron micrograph of a 2 μm long nanowire connected by tapered waveguide sections for input and output coupling. (b) Near-field amplitude of forward-propagating waves in the structure at $\lambda = 1550$ nm. The intensity transmission of the complete structure is $20 \pm 6\%$.

Grating-coupling of surface plasmons onto metallic tips: A nano-confined light source

Nano Lett. **7**, 2784-2788 (2007).

C. Ropers[1,*], C. C. Neacsu[1,2], T. Elsaesser[1], M. Albrecht[3],
M. B. Raschke[1,2], and C. Lienau[4]
[1] *Max-Born-Institut für Nichtlineare Optik und Kurzzeitspektroskopie, D-12489 Berlin, Germany*

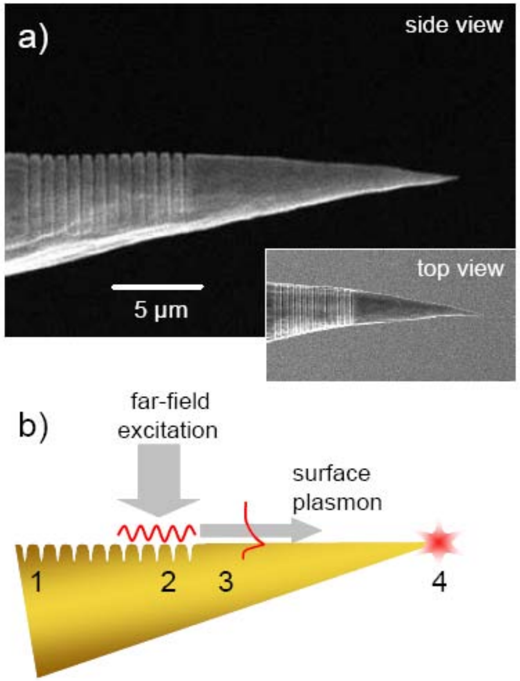

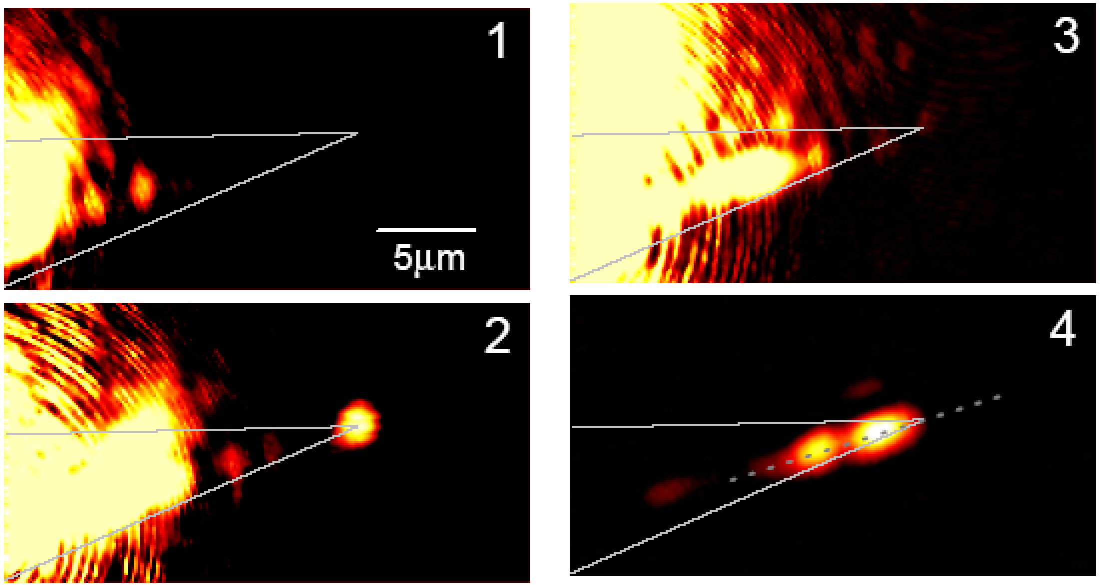

NANO LETTERS
pubs.acs.org/NanoLett

Near-Field Localization in Plasmonic Superfocusing: A Nanoemitter on a Tip

DOI: 10.1021/nl903574a | *Nano Lett.* **2010**, *10*, 592-596

Catalin C. Neacsu,[†,#] Samuel Berweger,[†,#] Robert L. Olmon,[†,‡,#] Laxmikant V. Saraf,[||] Claus Ropers,[⊥] and Markus B. Raschke*[,†,§]

[†]Department of Chemistry, [‡]Department of Electrical Engineering, [§]Department of Physics, University of Washington, Seattle, Washington 9819
Laboratory, Richland, Washington 9935
University of Göttingen, Germany

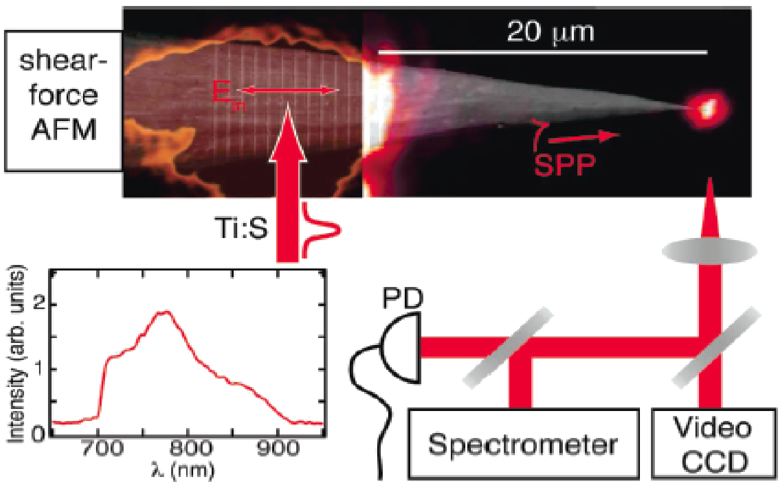

FIGURE 1. Grating coupling of surface plasmons on a tip. Overlay of SEM and optical far-field image of a Au tip with grating written by FIB for surface plasmon coupling of incident near-IR light from a Ti:Sapphire laser (spectrum shown). The grating with period $a_0 \sim$ 770 nm is illuminated with polarization parallel with respect to the tip axis and an incident focus size of $\sim$8 μm. The nonradiative SPP propagation leads to energy transfer and focusing and finally reemission near the tip apex with radius $\lesssim$15 nm.

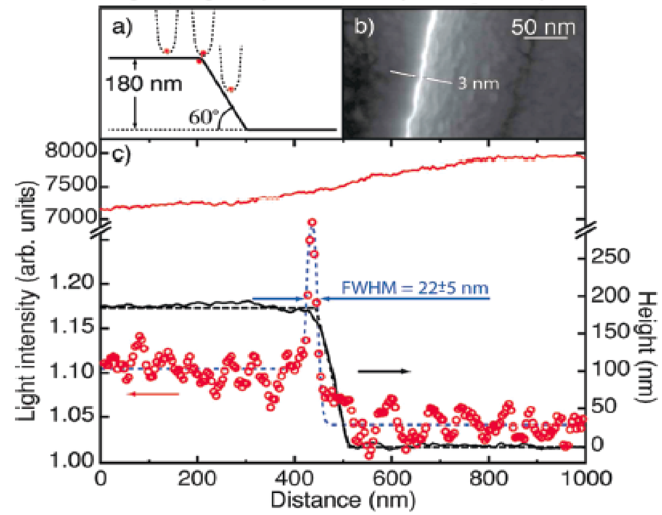

FIGURE 3. Determination of tip emitter size. (a) Schematic of scanning the nanofocusing tip across a silicon step edge with radius 3 ± 1 nm. (b) Top view SEM image of step edge. The wall and lower terrace are on the right-hand side. The edge serves as a local scatterer of the optical near-field of the apex. (c) The optical signal of a lateral scan across the step edge provides a measure of the spatial field confinement and thus the emitter size at the apex. Solid black line: AFM topography of the step. Red circles: plasmonic edge-scattered light intensity of the apex. The optical intensity peaks at the step edge and displays a width of 22 ± 5 nm, demonstrating the near-field localization at the apex. Solid red: Signal obtained under direct illumination of the apex under otherwise identical conditions.

LETTER
pubs.acs.org/NanoLett
dx.doi.org/10.1021/nl1045457 | *Nano Lett.* 2011, 11, 1609–1613

Adiabatic Nanofocusing Scattering-Type Optical Nanoscopy of Individual Gold Nanoparticles

Diyar Sadiq,[†] Javid Shirdel,[†] Jae Sung Lee,[‡] Elena Selishcheva,[†] Namkyoo Park,[‡] and Christoph Lienau*[,†]

[†]Institut für Physik, Carl von Ossietzky Universität, 26111 Oldenburg, Germany
[‡]Photonic Systems Laboratory, School of EECS, Seoul National University, Seoul 151-744, Korea

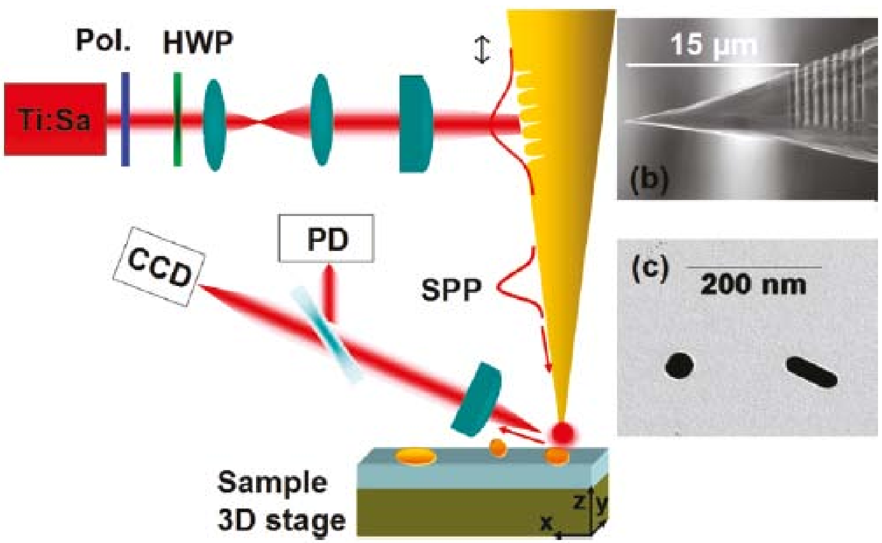

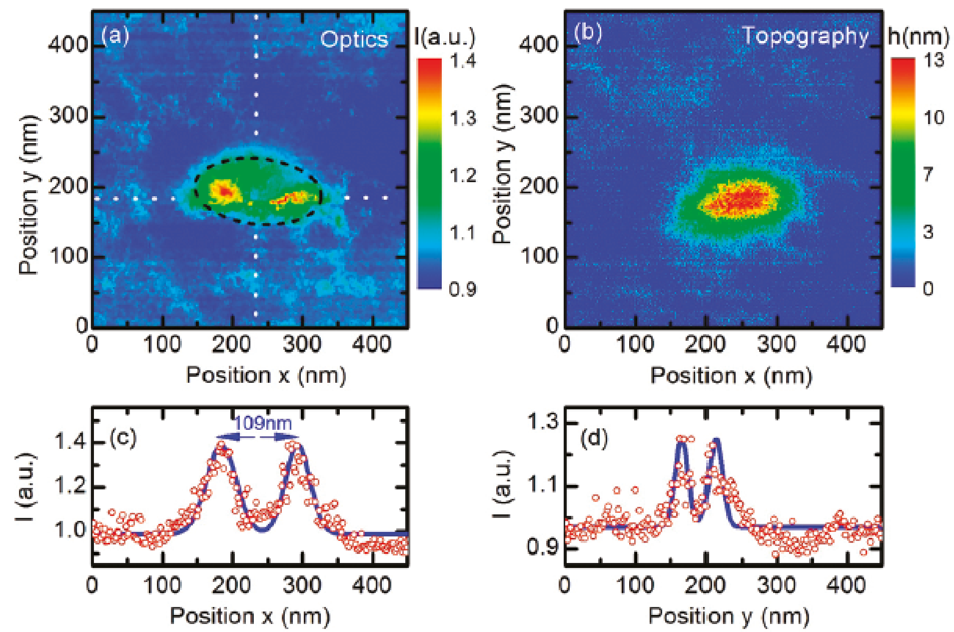

Figure 3. (a) Two-dimensional adiabatically focused s-NSOM image of an elliptical gold nanoparticle with $100 \times 40 \times 15\ \mathrm{nm}^3$ dimensions on a glass substrate. (b) Corresponding shear-force topographical image of the elliptical gold nanoparticle. (c,d) Cross sections of the optical intensity along the *x*- and *y*-directions (along the dashed lines in panel a). The strong near-field enhancement at the edges of both the long and short axis of the nanoparticle indicates that the component of the local electric field oriented along the tip axis (*z*-direction) is imaged.

Department of Physics and Astronomy
Georgia State University
Atlanta, GA 30303-3083

Di Fabrizio, E., *et. al*, Italian patent n. TO2008A000693 23.09.2008

5 nm radius

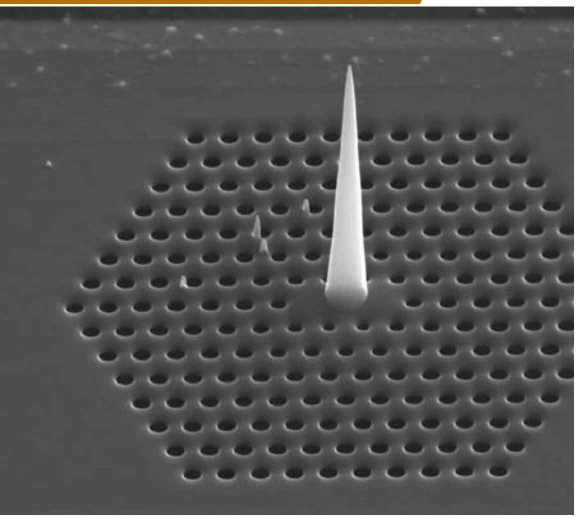

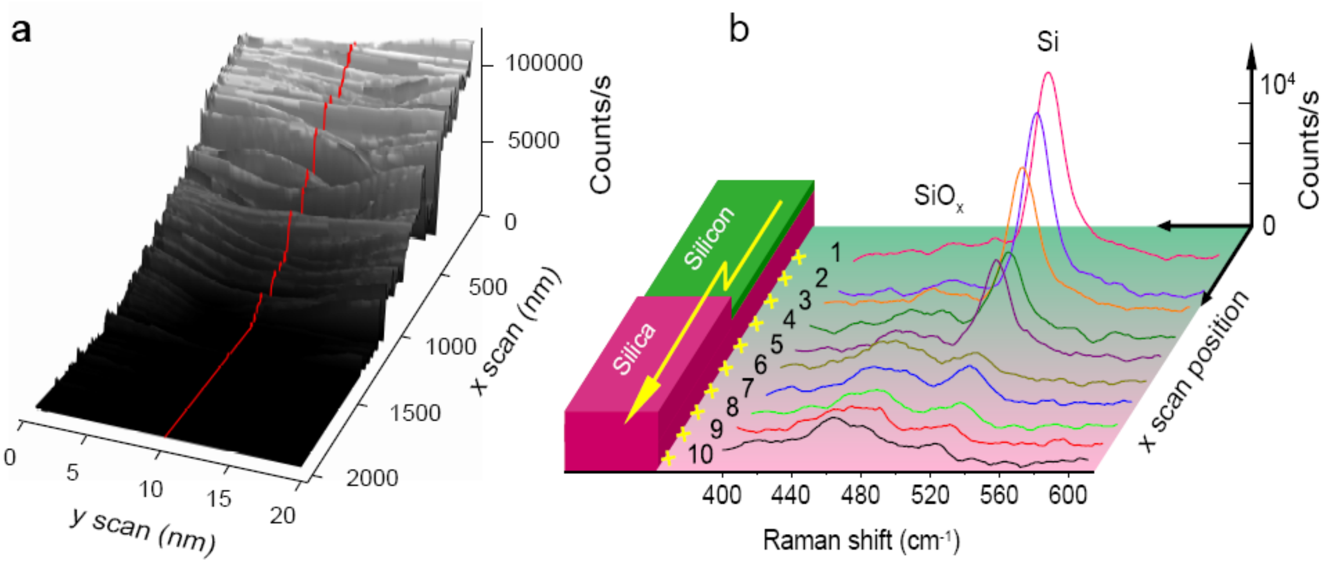

nature nanotechnology
ARTICLES
PUBLISHED ONLINE: 22 NOVEMBER 2009 | DOI: 10.1038/NNANO.2009.348

Nanoscale chemical mapping using three-dimensional adiabatic compression of surface plasmon polaritons

Francesco De Angelis[1,2], Gobind Das[1], Patrizio Candeloro[2], Maddalena Patrini[3], Matteo Galli[3], Alpan Bek[4], Marco Lazzarino[4,5], Ivan Maksymov[3], Carlo Liberale[2], Lucio Claudio Andreani[3] and Enzo Di Fabrizio[1,2*]

Adiabatic Nanofocusing Conclusions

•Due to adiabaticity, the back reflection and 3D scattering of SPP is minimal.

•The high wave vector of the TM0 SPP makes them dark (no coupling to the far field radiation).

•The velocity of SPP tends to zero proportionally to *R* as they approach the tip: *adiabatic slowing down and asymptotic stopping*.

•This leads to the accumulation of the SPP near the tip and their *adiabatic nanofocusing*.

•Under realistic conditions it is possible to transfer to the tip vicinity ~50% of the initial energy flux, that along with adiabatic stopping leads to the local field-intensity enhancement by three orders of magnitude

•The energy and optical field concentration at the tip of a taper is usable to excite a high-sensitivity, low-background SERS from a few molecules

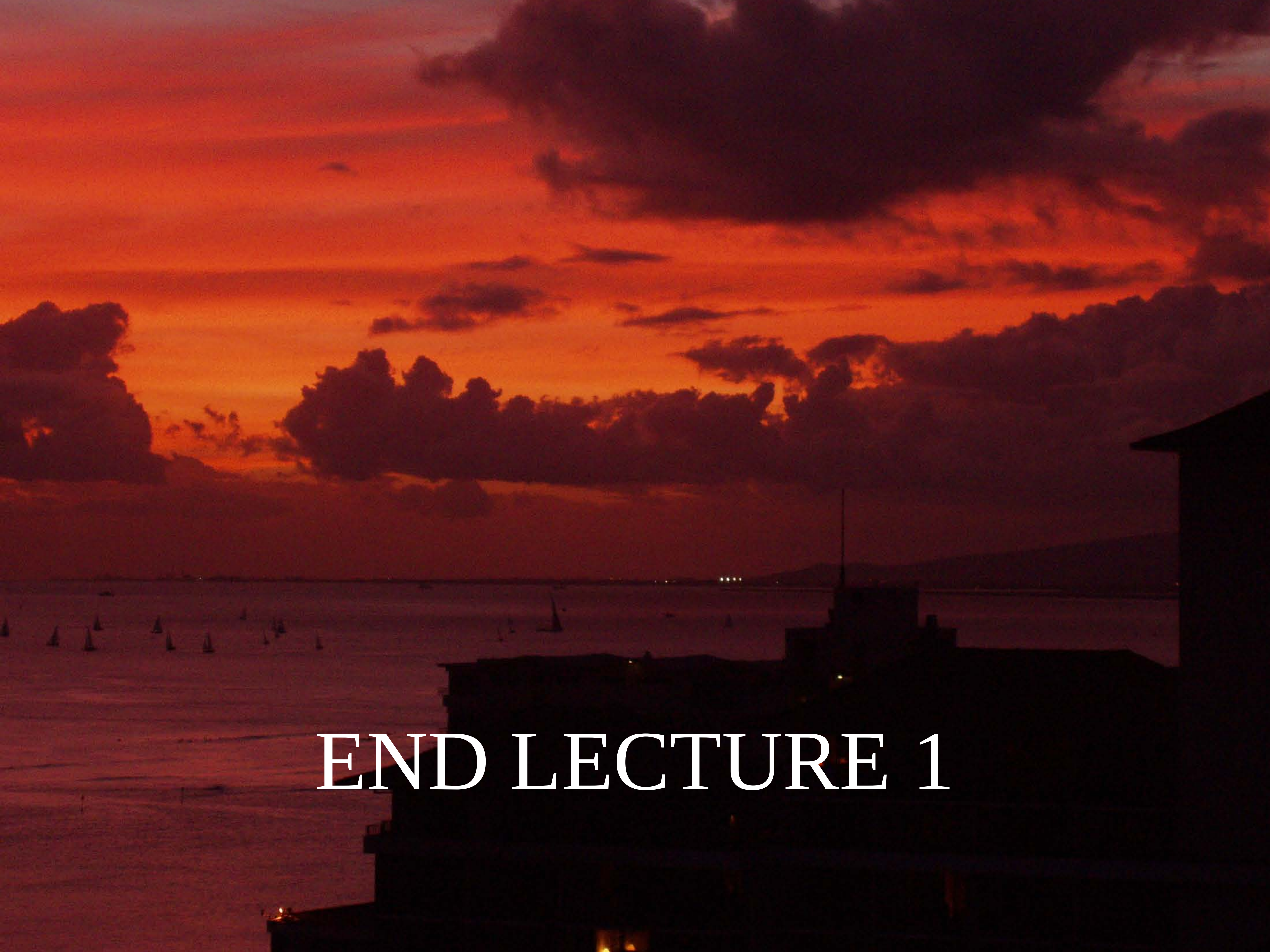
END LECTURE 1